Atmos. Chem. Phys. Discuss., https://doi.org/10.5194/acp-2017-626
Manuscript under review for journal Atmos. Chem. Phys.
Discussion started: 23 August 2017

Atmospheric Chemistry and Physics Discussions

Open burning of rice, corn and wheat straws: primary emissions, photochemical aging, and secondary organic aerosol formation

Zheng Fang[1,3], Wei Deng[1,3], Yanli Zhang[1,2], Xiang Ding[1], Mingjin Tang[1], Tengyu Liu[1], Qihou Hu[1], Ming Zhu[1,3], Zhaoyi Wang[1,3], Weiqiang Yang[1,3], Zhonghui Huang[1,3], Wei Song[1,2], Xinhui Bi[1], Jianmin Chen[4], Yele Sun[5], Christian George[6], Xinming Wang[1,2,*]

[1]State Key Laboratory of Organic Geochemistry and Guangdong Key Laboratory of Environment Protection and Resources Utilization, Guangzhou Institute of Geochemistry, Chinese Academy of Sciences, Guangzhou 510640, China

[2]Center for Excellence in Regional Atmospheric Environment, Institute of Urban Environment, Chinese Academy of Sciences, Xiamen 361021, China

[3]University of Chinese Academy of Sciences, Beijing 100049, China

[4]Shanghai Key Laboratory of Atmospheric Particle Pollution and Prevention, Department of Environmental Science & Engineering, Fudan University, Shanghai 200433, China

[5]Institute of Atmospheric Physics, Chinese Academy of Sciences, Beijing 100029, China

[6]Institut de Recherches sur la Catalyse et l'Environment de Lyon (IRCELYON), CNRS, UMR5256, Villeurbanne F-69626, France

Correspondence to: X. Wang (wangxm@gig.ac.cn)

Atmos. Chem. Phys. Discuss., https://doi.org/10.5194/acp-2017-626
Manuscript under review for journal Atmos. Chem. Phys.
Discussion started: 23 August 2017

Abstract. Agricultural residues are among the most abundant biomass burned globally, especially in China. However, there is rare information on primary emissions and photochemical evolution of agricultural residues burning. In this study, indoor chamber experiments were conducted to investigate primary emissions from open burning of rice, corn and wheat straws and their photochemical aging as well. Emission factors of NO_x, NH_3, SO_2, 67 non-methane hydrocarbons (NMHCs), particulate matter (PM), organic aerosol (OA) and black carbon (BC) under ambient dilution conditions were determined. Olefins accounted for >50% of the total NMHCs emission (2.47 to 5.04 g kg^{-1}), indicating high ozone formation potential of straw burning emissions. Emission factors of PM (3.73 to 6.36 g kg^{-1}) and primary organic carbon (POC, 2.05 to 4.11 gC kg^{-1}), measured at dilution ratios of 1300 to 4000, were lower than those reported in previous studies at low dilution ratios, probably due to the evaporation of semi-volatile organic compounds under high dilution conditions. After photochemical aging with OH exposure range of (1.97-4.97)×10^{10} molecule cm^{-3} s in the chamber, large amounts of secondary organic aerosol (SOA) were produced with OA mass enhancement ratios (the mass ratio of total OA to primary OA) of 2.4-7.6. The 20 known precursors could only explain 5.0-27.3% of the observed SOA mass, suggesting that the major precursors of SOA formed from open straw burning remain unidentified. Aerosol mass spectrometry (AMS) signaled that the aged OA contained less hydrocarbons but more oxygen- and nitrogen-containing compounds than primary OA, and carbon oxidation state (OS_c) calculated with AMS resolved O/C and H/C ratios increased linearly (p<0.001) with OH exposure with quite similar slopes.

Atmos. Chem. Phys. Discuss., https://doi.org/10.5194/acp-2017-626
Manuscript under review for journal Atmos. Chem. Phys.
Discussion started: 23 August 2017

Atmospheric Chemistry and Physics Discussions

1 Introduction

On the global scale, biomass burning (BB) is the main source of primary organic carbon (OC) (Bond et al., 2004; Huang et al., 2015), black carbon (BC) (Cheng et al., 2016), and brown carbon (BrC) (Laskin et al., 2015). It is also the second largest source of non-methane organic gases (NMOGs) in the atmosphere (Yokelson et al., 2008; Stockwell et al., 2014). In addition, atmospheric aging of biomass burning plumes produces substantial secondary pollutants. The increase of tropospheric ozone (O_3) in aged biomass burning plumes could last for days and even months (Thompson et al., 2001; Duncan et al., 2003; Real et al., 2007) with complex atmospheric chemistry (Arnold et al., 2015; Müller et al., 2016). Moreover, biomass and biofuel burning could contribute up to 70% of global secondary organic aerosols (SOA) burden (Shrivastava et al., 2015) and hence influence the seasonal variation of global SOA (Tsigaridis et al., 2014). Since it produces large amounts of primary and secondary pollutants, it is essential to characterize primary emissions and photochemical evolution of biomass burning in order to better understand its impacts on air quality (Huang et al., 2014), human health (Alves et al., 2015) and climate change (Andreae et al., 2004; Koren et al., 2004; Laskin et al., 2015; Huang et al., 2016).

Open burning of agricultural residues, a convenient and inexpensive way to prepare for the next crop planting, could induce severe regional haze events (Cheng et al., 2013; Tariq et al., 2016). Among all the biomass burning types, agricultural residues burning in the field is estimated to contribute ~10% of the total mass burned globally (Andreae and Merlet, 2001), and its relative contribution is even larger in Asia (~34%) and especially in China (>60%) (Streets et al., 2003) where >600 million people live in the countryside (NBSPRC, 2015). Agricultural residues burned in China were estimated to be up to 160 million tons in 2012, accounting for ~40% of the global agricultural residues burned (Li et al., 2016). As estimated by Tian et al. (2011), agricultural residues burning contributed to 70-80% of non-methane

hydrocarbons (NMHCs) and particulate matter (PM) emitted by biomass burning in China during 2000-2007. A better understanding of the role agricultural residual burning plays in air pollution in China and elsewhere requires better characterization of primary emission and atmospheric aging of emitted trace gases and particles for different types of agricultural residues under different burning conditions.

In the pasted two decades, there have been increasing numbers of characterization of biomass burning emissions. Andreae and Merlet (2001) summarized emission factors (EFs) for both gaseous and particulate compounds from seven types of biomass burning. Akagi et al. (2011) updated the emission data for fourteen types of biomass burning, and newly identified species were included. Since biomass types and combustion conditions may differ in different studies, reported emission factors are highly variable, especially for agricultural residues burning (Li et al., 2007; Cao et al., 2008; Zhang et al., 2008; Li et al., 2009; Yokelson et al., 2011; Brassard et al., 2014; Sanchis et al., 2014; Wang et al., 2014; Ni et al., 2015; Kim Oanh et al., 2015; Li et al., 2017). Moreover, previous studies on agricultural residues burning were mostly carried out near fire spots or in chambers with low dilution ratios. Since biomass burning organic aerosols (BBOA) are typically semi-volatile (Grieshop et al., 2009b; May et al., 2013), it is expected that measured BBOA emission factors would be affected by dilution processes (Lipsky et al., 2006), and BBOA emission factors under ambient dilution conditions are still unclear. Furthermore, knowledge in NMOGs emitted from agricultural residues burning is very limited. As reported by Stockwell et al. (2015), ~21% (in weight) of NMOGs in biomass burning plumes have not been identified yet. Therefore, comprehensive measurement and characterization of gaseous and particulate species emitted by agricultural residues burning under ambient dilution conditions are urgently needed.

Great attention has been drawn to SOA formation and transformation in biomass burning plumes recently, since significant increase of mass and apparent change in physicochemical

characteristics of aerosols have been observed during atmospheric aging of biomass burning plumes in both field and laboratory studies (Grieshop et al., 2009a,b; Hennigan et al., 2011; Heringa et al., 2011; Lambe et al., 2011; Jolleys et al., 2012; Giordano et al., 2013; Martin et al., 2013; Ortega et al., 2013; Ding et al., 2016a; Ding et al., 2016b; Ding et al., 2017). For agricultural residues burning, evolution processes have not been well characterized yet. To our knowledge, up to now there is only a chamber study (Li et al., 2015) which has investigated the evolution of aerosol particles emitted by wheat straw burning under dark conditions. Although field studies (Adler et al., 2011; Liu et al., 2016) witnessed the evolution in mass concentrations, size distribution, oxidation state and optical properties of aerosol particles emitted by agricultural residues burning, these changes could be also influenced by other emission sources and meteorological conditions as well. Since NMOGs emitted by agricultural residues burning are not fully quantified, it is still challenging to predict the concentration and physicochemical properties of SOA resulted from biomass burning (Spracklen et al., 2011; Jathar et al., 2014; Shrivastava et al., 2015). Bruns et al. (2016) suggsted that the 22 major NMOGs identified in residential wood combustion could explain the majority of observed SOA, but it remains unclear whether identified NMOGs emitted by agricultural residues burning could fully (or at least largely) explain the SOA formed. In addition, aerosol mass spectrometry (AMS) has been widely used to characterize sources and evolution of ambient OA (Zhang et al., 2011). Although agricultural residues burning is an important type of biomass burning in Asia and especially in China, the lack of AMS spectra for primary and aged OA from agricultural residues burning significantly limits further application of AMS in BBOA research.

In this study, plumes from agricultural residues open burning were directly introduced into a large indoor chamber to firstly characterize primary emissions and then investigate their photochemical evolution under ~25°C and ~50% relative humidity. Corn, rice and wheat straws, which accounts for more than 90% of the crop residues burned in China (FAO, 2017), were

chosen. A suite of advanced online and offline techniques were utilized to measure gaseous and particulate species, enabling comprehensive measurements of emission factors of gaseous and particulate compounds for burning of each types of straw under ambient dilution conditions. In addition, corresponding formation and transformation of SOA during photochemical aging was investigated using a large indoor smog chamber. This work would help improve our understanding of primary emission, SOA formation and thus environmental impacts of agricultural residues burning.

2 Materials and methods

2.1 Experimental setup

Photochemical aging was investigated in a smog chamber in the Guangzhou Institute of Geochemistry, Chinese Academy of Sciences (GIG-CAS). The GIG-CAS smog chamber is a ~30 m^3 fluorinated ethylene propylene (FEP) reactor housed in a temperature-controlled room. Details of the chamber setup and associated facilities are provided elsewhere (Wang et al., 2014; Liu et al., 2015, 2016; Deng et al., 2017). Briefly, 135 black lamps (1.2 m long, 60 W Philips, Royal Dutch Philips Electronics Ltd, the Netherlands) are used as light sources, giving a NO_2 photolysis rate of approximately 0.25 min^{-1}. Two Teflon-coated fans are installed inside the reactor to ensure introduced gaseous and particulate species mixed well within 2 min. Prior to each experiment, the reactor was flushed with purified dry air at a rate of 100 L min^{-1} for at least 48 h.

Corn, rice and wheat straws were collected from Henan, Hunan and Guangdong province, respectively. Since moisture content in straws would affect emission factors of atmospheric pollutants (Sanchis et al., 2014; Ni et al., 2015), all the agricultural residues used in this study were dried in a stove at 80 °C for 24 h before being burned. After baking, water content in the crop residues was less than 1%. In each experiment, ~300 g straws were burned and the burning typically lasted for 3-5 min. Straws were ignited by a butane-fueled lighter and burned under

open field burning conditions. The resulting smoke was collected by an inverted funnel and introduced into the chamber using an oil-free pump (Gast Manufacturing, Inc, USA) at a flow rate of ~15 L min^{-1} through a 5.5 m long copper tube (inner diameter: 3/8 inch), and the residence time in the tube was estimated to be <2 s. Before each experiment, the transfer tube was pre-flushed for 15 min with ambient air and 2 min with smokes (not introduced into the chamber reactor). During the whole process, the tube was heated at 80 °C to reduce the losses of organic vapors. Based on the volumes of the smoke introduced and the chamber reactor, the dilution ratios were estimated to be 1300-4000, falling into the typical range (1000-10000) under ambient dilution conditions (Robinson et al., 2007). After being characterized in dark for >20 min, black lumps were turned on and the diluted smoke were photochemically aged for 5 h. At the end, black lamps were switched off and the aged aerosols were characterized in the next one hour to correct the particle wall loss.

In total 20 experiments were conducted (9 for rice straw, 6 for corn straw and 5 for wheat straw), among which 14 experiments were conducted only in the dark to measure primary emissions and 6 experiments were carried out both in the dark and under irradiation to investigate photochemical evolution of open straw burning emissions. Tables 1 and 2 summarize important experimental conditions and key results for all the experiments.

2.2 Instrumentation

Gaseous and particulate species were monitored with a suite of online and offline instruments. Commercial instruments were used for online monitoring of NO_x (EC9841T, Ecotech, Australia), NH_3 (Model 911-0016, Los Gatos Research, USA) and SO_2 (Model 43i, Thermo Scientific, USA). Volatile organic compounds (VOCs) were continuously measured using a proton-transfer-reaction time-of-flight mass spectrometer (PTR-TOF-MS; Model 2000, Ionicon Analytik GmbH, Austria). Calibration of the PTR-TOF-MS was performed every few weeks using a certified custom-made standard mixture of VOCs (Ionicon Analytik Gmbh,

Austria) that were dynamically diluted to 6 levels (2, 5, 10, 20, 50 and 100 ppbv). Methanol, acetonitrile, acetaldehyde, acrolein, acetone, isoprene, crotonaldehyde, 2-butanone, benzene, toluene, o-xylene, chlorobenzene and α-pinene were included in the calibration mixture. Their sensitivities, indicated by the ratio of the normalized counts per second to the concentration levels of the VOCs in ppbv, were used to convert the raw PTR-TOF-MS signal to concentration (Huang et al., 2016). Quantification of the compounds that were not included in the mixture was performed by using calculated mass-dependent sensitivities based on the measured sensitivities (Stockwell et al., 2015). Mass-dependent sensitivities were linearly fitted for oxygen-containing compounds and the remaining compounds separately. The decay of toluene measured by PTR-TOF-MS was used to derive the OH radical concentrations for every 2 min during each experiment, and the OH exposure was calculated as the product of the OH concentration and the time interval. Air samples were also collected from the chamber reactor using 2-Liter electro-polished stainless-steel canisters before and after smoke injection. In total 67 C_2-C_{12} NMHCs were measured (Table S1) using an Agilent 5973N gas chromatography mass-selective detector/flame ionization detector (GC-MSD/FID; Agilent Technologies, USA) coupled to a Preconcentrator (Model 7100, Entech Instruments Inc., USA), and analytical procedures have been detailed elsewhere (Wang and Wu, 2008; Zhang et al., 2010; Zhang et al., 2012). CH_4 and CO were analyzed using a gas chromatography (Agilent 6980GC, USA) coupled with a flame ionization detector and a packed column (5A molecular sieve 60/80 mesh, 3 m × 1/8 in) (Zhang et al., 2012), and CO_2 was analyzed using a HP 4890D gas chromatograph (Yi et al., 2007). The detection limits were all less than 30 ppbv for CH_4, CO and CO_2. The relative standard deviations (RSDs) of CO and CO_2 measurements were both less than 3% based on seven duplicate injection of 1.0 ppmv standards (Spectra Gases Inc, USA).

Particle number/volume concentrations and size distribution were measured with a scanning mobility particle sizer (SMPS; Classifier model 3080, CPC model 3775, TSI

Incorporated, USA). The SMPS was operated with a sheath flow of 3.0 L min^{-1} and a sampling flow of 0.3 L min^{-1}, allowing for a size scanning range of 14 to 760 nm within 255 s. A high-resolution time-of-flight aerosol mass spectrometer (HR-TOF-AMS; Aerodyne Research Incorporated, USA) was used to measure chemical compositions of non-refractory aerosol particles (DeCarlo et al., 2006). The instrument alternated every one min between the high sensitivity V mode and the high resolution W mode. The toolkit Squirrel 1.57I was used to obtain real-time concentration variations of sulfate, nitrate, ammonium, chloride and organics, and the toolkit Pika 1.16I was used to determine the detailed compositions of OA (Aiken et al., 2007; Aiken et al., 2008; Canagaratna et al., 2015). The AMS signal at m/z 44 was corrected for the contribution from gaseous CO_2. Ionization efficiency of the AMS was calibrated routinely by measuring 300 nm monodisperse ammonium nitrate particles. Considering the underestimation of particulate matter by AMS, aerosol mass measured by AMS was corrected with the data from the SMPS and the aethalometer. Conductive silicon tubes were used for aerosol sampling to reduce electrostatic losses of particles.

BC was measured with a seven-channel aethalometer (Model AE-31, Magee Scientific, USA). Cheng et al. (2016) measured the mass absorption efficiency (MAE) of BC from biomass burning at wavelengths of 532 and 1047 nm respectively, and the absorption Ängström exponents (AAE) were estimated to be in the range of 0.9-1.1. Based on relationship between MAE and wavelength, a MAE value of 4.7 m^2 g^{-1} was calculated for 880 nm by assuming the AAE to be 1.0. The MAE value was then applied to convert absorption data in 880 nm to BC mass concentrations. Aethalometer attenuation measurements were corrected for particle loading effects and the scattering of filter fibers using the method developed by Kirchstetter and Novakov (2007) and Schmid et al. (2006).

Atmos. Chem. Phys. Discuss., https://doi.org/10.5194/acp-2017-626
Manuscript under review for journal Atmos. Chem. Phys.
Discussion started: 23 August 2017

Atmospheric Chemistry and Physics Discussions

2.3 Data analysis

2.3.1 Particle effective density

Assuming that particles are spherical and non-porous, the effective density (ρ_{eff}) can be estimated by Eq. (1) (DeCarlo et al. 2004; Schmid et al. 2007):

$$\rho_{eff}=\rho_0 \cdot \frac{d_{va}}{d_m} \quad (1)$$

where ρ_0 is the standard density (1.0 g cm^{-3}), and d_{va} and d_m are the AMS-measured vacuum aerodynamic diameter and SMPS-measured mobility diameter. The input diameters to this equation were determined by comparing distributions of vacuum aerodynamic and electric mobility diameters, using the AMS and SMPS respectively. Derived ρ_{eff} was used to convert volume concentrations of aerosol particles measured by the SMPS to mass concentrations.

2.3.2 Emission factors and modified combustion efficiency

The carbon mass balance approach (Ward et al., 1992; Andreae and Merlet, 2001) was used to calculate fuel based emission factors (EF) for each compound (g kg^{-1} dry fuel). The emission factor for the *i*th species, EF_i, is calculated by Eq. (2):

$$EF_i=\frac{m_i \cdot EF_C}{\Delta[CO_2]+\Delta[CO]+\Delta[PM_C]+\Delta[HC]} \quad (2)$$

where m_i is the concentration (g m^{-3}) of the *i*th species; $\Delta[CO_2]$, $\Delta[CO]$, and $\Delta[HC]$ are the background-corrected carbon mass concentration (g-C m^{-3}) of the CO_2, CO, and hydrocarbons, respectively; $\Delta[PM_C]$ is the background-corrected carbon in the particle phase (g-C m^{-3}); EF_C is the emission factor of carbon into the air determined by elemental analysis, given by Eq. (3):

$$EF_C=\frac{m_{fuel} \cdot \omega_{fuel}-m_{ash} \cdot \omega_{ash}}{m_{fuel}} \quad (3)$$

where ω_{fuel} and ω_{ash} are mass fractions of carbon in the dry fuel and its ash, and m_{fuel} and m_{ash} are the mass of dry fuel and its ash. The modified combustion efficiency (MCE) is defined by Eq. (4) (Heringa et al., 2011; Hennigan et al., 2011; Ni et al., 2015):

$$MCE=\frac{\Delta[CO_2]}{\Delta[CO_2]+\Delta[CO]} \quad (4)$$

Atmos. Chem. Phys. Discuss., https://doi.org/10.5194/acp-2017-626
Manuscript under review for journal Atmos. Chem. Phys.
Discussion started: 23 August 2017

2.3.3 Ozone formation potential

The ozone formation potential (OFP) of NMHCs was calculated from the emission factor and maximum incremental reactivity (MIR) of each individual NMHCs, using Eq. (5):

$$OFP = \sum_{i=1}^{n} (EF_i \cdot MIR_i) \qquad (5)$$

where OFP is the ozone formation potential of NMHCs emitted from per unit of biomass (unit: g kg^{-1}), and MIR_i is the MIR of the *i*th NMHC (unit: g O_3 per g NMHC) (Carter 2008).

2.3.4 Wall loss corrections

Due to the loss of particles and vapors to chamber walls, measured data in chamber studies need to be corrected for wall loss. For this purpose, in our study one-hour dark decay of aged aerosols was undertaken after photochemical aging was terminated. The loss of particles on the chamber wall is a first-order process (McMurry and Grosjean, 1985). The wall-loss rates of AMS-measured organics, sulfate, nitrate, chloride and ammonium were determined using the dark decay data and were applied to wall-loss correction for the entire experiment. By assuming that the condensed materials on the wall remains completely in equilibrium with the gas phase, we used the ω=1 case to correct the OA mass, where ω is a proportionality factor of organic vapor partitioning to chamber walls and suspended particles (Weitkamp et al., 2007; Henry et al., 2012). For SMPS measurements, the number concentration in each size channel (110 channels in total) was corrected for wall loss separately, since wall loss rates of aerosol particles are size-dependent (Takekawa et al., 2003).

2.3.5 OA production prediction

In this study, twenty NMOGs which have been used to estimate SOA yields by previous work (Ng et al., 2007b; Chan et al., 2009; Hildebrandt et al., 2009; Gómez Alvarez et al., 2009; Chan et al., 2010; Shakya and Griffin, 2010; Chhabra et al., 2011; Nakao et al., 2011; Borras and Tortajada-Genaro, 2012; Yee et al., 2013; Lim et al., 2013) were identified using PTR-TOF-MS, and the applied SOA yields are summarized in Table S2. The mass concentration of SOA

266 ($[SOA]_{predicted}$, μg m^{-3}) formed from these twenty precursors can be estimated using Eq. (6):

267 $$[SOA]_{predicted} = \sum_i (\Delta[X_i] \cdot Y_i) \quad (6)$$

268 where $\Delta[X_i]$ (μg m^{-3}) is the reacted amount of the *i*th gas-phase precursor and Y_i is the
269 corresponding SOA yield.

270 Assuming that primary OA (POA) levels kept constant during aging processes, the mass
271 concentration of SOA formed could be estimated as the difference in OA mass concentrations
272 before and after photochemical aging. It should be noted that POA would decrease during aging
273 processes (Tiitta et al., 2016), probably leading to the underestimation of the formed SOA. In
274 papers where those SOA yields were borrowed from, no organic vapor wall loss were
275 accounted for when calculating the mass concentration of the formed SOA, so the same wall
276 loss correction method was used when comparing the predicted SOA and the formed SOA.

277 **3 Results and discussion**

278 **3.1 Emissions of gaseous pollutants**

279 Table 1 compares emission factors of gaseous and particulate species measured in our and
280 previous studies. In our study, emission factors of NO_x were 1.47±0.61, 5.00±3.94, and
281 3.08±0.93 g kg^{-1} for rice, corn and wheat straw, and NO accounted for 84±11% of NO_x primary
282 emission for all experiments. Emission factors of NH_3 were measured to be 0.45±0.15,
283 0.63±0.30 and 0.22±0.19 g kg^{-1} for rice, corn and wheat straw. Our measured emission factors
284 of reactive nitrogen species were comparable to those reported by previous studies (Li et al.
285 2007; Tian et al. 2011). Emission factors of SO_2 were 0.07±0.07, 0.99±1.53 and 0.72±0.34 g
286 kg^{-1} for rice, corn and wheat straw. Our measured emission factors of SO_2 were lower than
287 those reported by Cao et al., (2008) and Kim Oanh et al. (2015) for rice straw, but higher those
288 reported by Cao et al., (2008) for corn and wheat straw. Due to low sulfur contents in crop
289 straws, the SO_2 emission factors for open burning of crop residues were much lower than those
290 for coal combustion, which were determined to be 9.92±2.83 g kg^{-1} for household combustion

of coal cakes (Ge et al., 2004).

Emission factors of NMHCs were 5.04±2.04, 2.47±2.11 and 3.08±2.43 g kg^{-1} for rice, corn and wheat straw, respectively (Table 1). Our results were higher than those reported by previous studies (Li et al., 2009; Wang et al., 2014), partly due to the fact that more NMHCs were analyzed in our study (67 species in total). As shown in Figure 1a-c, olefins and acetylene accounted for 56-58% of the total NMHCs, followed by alkanes (22-28%) and aromatic hydrocarbons (16-21%). Table S1 and Figure 2 show the emission factors of each NMHC for open burning of different straws. Emission factors of unsaturated hydrocarbons ranged from 1.37 (corn) to 2.91 g kg^{-1} (rice), with the majority being ethene, acetylene and propene. Emission factors of alkanes ranged from 0.69 (corn) to 1.09 g kg^{-1} (rice), with ethane and propane being the two most abundant compounds. The emission factors of aromatic hydrocarbons were in the range of 0.42 (corn) to 1.04 (rice), and benzene and toluene are dominant species. It is worth noting that major compounds in the three groups (alkanes, alkenes and aromatic hydrocarbons) were all negatively correlated with the modified combustion efficiency (Figure S1), suggesting that more efficient combustion would reduce their emissions.

Based on their emission factors, we calculated the ozone formation potential for each NMHC. The summed ozone formation potential were 22.5±10.1, 13.7±12.4 and 16.3±13.5 g kg^{-1} for open burning of rice, corn and wheat straw, respectively. As shown in Figure 1d-e, the relative contributions of olefins to the total ozone formation potential could reach >80%. Ethene was the largest ozone precursor (35-42%), followed by propene (16-28%), and these two compounds contributed 58-64% of the total ozone formation potential. Although the emission factors of aromatic hydrocarbons were lower than those of alkanes, their ozone formation potential was dominant over those of alkanes, with toluene being the largest contributor among all the aromatic hydrocarbons. The contribution of alkanes to the total ozone formation potential was minor (2-3%).

Atmos. Chem. Phys. Discuss., https://doi.org/10.5194/acp-2017-626
Manuscript under review for journal Atmos. Chem. Phys.
Discussion started: 23 August 2017

316 **3.2 Emission of particulate matters**

317 The emission factors of particulate matters were 3.73±3.28, 5.44±3.43, 6.36±2.98 g kg^{-1} for
318 rice, corn and wheat straw, lower than those reported in the previous studies (Table 1). As
319 suggested by Robinson et al. (2007), the POA emission factors would decrease with increasing
320 dilution ratios, due to evaporation of semi-volatile organic compounds. In this study, the
321 dilution ratios ranged from 1300 to 4000, which were within the typical range of ambient
322 dilution ratios (1000-10000) (Robinson et al. 2007). Therefore, it can be expected that emission
323 factors of primary organic carbon (POC) measured in our study (2.05-4.11 gC kg^{-1}) were lower
324 than those measured by previous work with dilution ratios of 5-20 (Li et al. 2007; Ni et al.
325 2015). Moreover, it has been shown that the modified combustion efficiency could affect
326 emission factors (Heringa et al., 2011; Stockwell et al., 2015). Figure S2 shows negative
327 correlations of the modified combustion efficiency with emission factors of PM and POC
328 (p<0.05 for both cases), indicating that enhancement of combustion efficiency could reduce
329 the emissions of PM and POC. In our study, all straws were pre-baked to reduce the moisture
330 content to <1%, and this treatment could increase the modified combustion efficiency and thus
331 reduce emission factors of particulate matters (Ni et al., 2015). In addition, the amount of straws
332 burned each time in our experiments was much less than that in the fields, which is expected
333 to avoid oxygen deficit during burning to some extent and thus increase the modified
334 combustion efficiency as well.

335 While POA emission factors showed large variability for different types of straw, BC
336 emission factors were relatively constant (0.22-0.27 gC kg^{-1}). Since BC is a mixture of non-
337 volatile compounds in particulate matters, as expected, its emission factors measured in our
338 work were comparable to those reported under lower dilution conditions (Li et al. 2007; Ni et
339 al. 2015). The Δ[POA]/Δ[CO] ratios ranged from 0.022 to 0.133 in our study, larger than those
340 (0.001-0.067) measured in chamber studies for hard- and soft-wood fires (Grieshop et al.,

2009b) and vegetation commonly burned in North American wildfires (Heringa et al., 2011), but lower than those (0.051-0.329) obtained in field campaigns (Jolleys et al., 2012).

For particle numbers, the emission factors were $(2.94\pm0.91)\times10^{15}$, $(7.29\pm4.17)\times10^{15}$, $(5.87\pm2.89)\times10^{15}$ particle kg^{-1} for rice, corn and wheat straw, respectively (Table 1). Our results were comparable to that (1×10^{15} particle kg^{-1}) for crop residues burning (Andreae and Merlet, 2001) and those (3.2×10^{15}-10.9×10^{15} particle kg^{-1}) for wood burning (Hosseini et al., 2013) but two magnitudes larger than those for crop residues burning in a sealed stove (Zhang et al. 2008).

3.3 Evolution of particles

3.3.1 Growth of particle size

Figure 3 shows the evolution of particle size distribution after photochemical aging of 0, 0.5, 2.5 and 5 h. Aerosol particles emitted from open straw burning were peaked at 40-80 nm under ambient dilution conditions. The geometric mean diameters for primarily emitted particles in this study were smaller than those (100-150 nm) reported for crop residuals burning under low dilution conditions (Zhang et al., 2011; Li et al., 2015), probabley due to evaporation of organic vapors under the high dilution conditions (Lipsky et al., 2006) and coagulation of fine particles under the low dilution conditions (Hossain et al., 2012).

After switching on black lamps, apparent growth of particle size was observed. In all the aging experiments, growth rates of particle diameters in the first 0.5 h were 10 times larger than those afterwards, and after 5 h aging the geometric mean diameters peaked at 60-120 nm. For instance, in the photochemical aging experiment for wheat straw burning (Figure 3c), the growth rate of particles was 18 nm h^{-1} in the first 0.5 h and decreased to ~1 nm h^{-1} during the following 4.5 h. The size distribution of aged aerosol particles in our study is similar to those of ambient particles under the severe biomass burning impact during haze events (Betha et al., 2014; Niu et al., 2016).

Atmos. Chem. Phys. Discuss., https://doi.org/10.5194/acp-2017-626
Manuscript under review for journal Atmos. Chem. Phys.
Discussion started: 23 August 2017

3.3.2 Particle mass enhancement

Figure 4 shows the chemical evolution of aerosol particles during the 5 h photochemical aging of wheat straw burning. During the whole process, OA kept increasing and was dominant over inorganic species. After 3 h of photochemical aging, the levels of all the inorganic species were constant, and nitrate was the second most abundant component with a mass fraction of 7%, followed by chloride (2%), ammonium (1%) and sulfate (<1%). Figure 4b depicts [OA] evolution as a function of OH exposure. OA increased slowly at the first ~0.2 h, and then increased rapidly with OH exposure.

The OA enhancement ratio, defined as the mass ratio of aged OA at the end of each aging experiment to POA, was calculated. In the six aging experiments, the OH exposure and OA enhancement ratios ranged from (1.87-4.97)×10^{10} molecule cm^{-3} s and 2.4-76, respectively. Assuming an average OH concentration of 1.5×10^{6} molecule cm^{-3} in the ambient air (Hayes et al., 2013), this means that rapid SOA formation would occur in 3.5-9.2 h during the daytime after straw burning. The OA enhancement ratios determined in our study were higher than those (0.7-2.9) for the combustion of vegetation commonly burned in North American wildfires (Hennigan et al., 2011), and comparable to those (0.7-6.9) for wood burning (Grieshop et al., 2009b; Heringa et al., 2011).

Recently, Bruns et al., (2016) found that 22 NMOGs emitted from residential wood burning could explain the majority of the formed SOA. In our study, 20 of the 22 NMOGs were detected and quantified with the PTR-TOF-MS. Concentration differences of each compound before and after photo-oxidation were calculated to estimate the SOA formed from these precursors. Since SOA formation highly depends on oxidation conditions, SOA yields for a certain precursor vary with VOC/NO_x ratios. In our work, we chose a set of SOA yields for these NMOGs based on the observed VOC/NO_x ratio in the chamber experiments. More specifically, if the observed VOC/NO_x ratio for a certain precursor in the chamber was within

the VOC/NO_x range reported in literature, the mean value of the highest and lowest yields within the VOC/NO_x range in literature was used to estimate the SOA formed from the precursor in the chamber; if the observed VOC/NO_x ratio for a certain precursor was higher than the maximum VOC/NO_x ratio reported in literature, we chose the yield reported at the maximum VOC/NO_x ratio; if the observed VOC/NO_x ratio was lower than the minimum VOC/NO_x ratio reported in literature, we chose the yield reported at the minimum VOC/NO_x ratio.

Figure 5a shows the time series of POA, $SOA_{predicted}$ and unexplained SOA in a typical aging experiment. The contribution of $SOA_{predicted}$ by the 20 NMOGs was minor, and large fractions of observed SOA could not be explained. In all the experiments, only 5.0-27.3% of the observed SOA mass could be explained by the 20 NMOGs (Figure 5b). Even if the highest SOA yield for each precursor reported in literature was used, 60-90% of observed SOA mass still could not be explained. It has been suggested that aqueous-phase oxidation of alkenes could produce substantial SOA (Ervens et al., 2011). Considering large emissions of olefins from straw burning (Figure 1a-c), we also estimated the SOA formed from the three most abundant alkenes (ethene, acetylene, and propene) with their newly-developed SOA yields (Ge et al., 2016; Jia and Xu, 2016; Ge et al., 2017), and their total contribution to the observed SOA was found to be negligible (<0.5%). Therefore, there are still unknown precursors and/or physicochemical processes contributing the majority of SOA formed from open straw burning.

3.3.3 OA mass spectrum evolution

In the high resolution W mode of AMS, ions generated from particles could be identified by their exact mass-charge ratio (m/z) and then grouped into CHON, CHO, CHN and CH families. Figure 6 presents the evolution of OA mass spectra. For POA (Figure 6a), CH-family was the major component with a mass fraction of 68%, followed by CHO (23%), CHN (6%), and CHON (2%). The ions at m/z 43, 41 and 55 were the dominant peaks in the POA mass spectrum.

Atmos. Chem. Phys. Discuss., https://doi.org/10.5194/acp-2017-626
Manuscript under review for journal Atmos. Chem. Phys.
Discussion started: 23 August 2017

Atmospheric Chemistry and Physics Discussions

The major ions at m/z 27, 39, 41, 55, 57, 67 and 69 belonged to the CH-family and could be the fragments of hydrocarbons (Weimer et al., 2008). The peaks at m/z 28, 29, 43, 44 and 55 contained considerable CHO ions, and the corresponding ions (CO^+, CHO^+, $C_2H_3O^+$, CO_2^+ and $C_3H_3O^+$) could be the fragments of aldehydes, ketones and carboxylic acid (Ng et al., 2011a). The peak at m/z 91 was mainly attributed to $C_7H_7^+$, possibly originating from aromatic compounds.

The mass spectra of aged OA was quite different from that of POA (Figure 6b-c). The mass fraction of the CH-family decreased to 46% and was comparable to that of CHO-family, while the contribution of N-containing OA (CHN and CHON) increased to ~11%. The ions at m/z 44 and 43, mainly coming from the CHO-family, became the dominant peaks for the aged OA. The fractions of two major masses at m/z 44 (f_{44}) and m/z 43 (f_{43}) in OA can be used to generate an f_{44} vs. f_{43} triangular space, in which oxygenated organic aerosol (OOA) moves towards the apex during the aging process (Ng et al., 2010). In addition, f_{44} in the ambient air was suggested to be 0.07±0.04 for semi-volatile OOA (SV-OOA) and 0.17±0.04 for low-volatility OOA (LV-OOA), respectively (Ng et al., 2010). Figure 7a plots f_{44} and f_{43} of the POA and the aged OA in all the six experiments. Most of data are within the f_{44} vs. f_{43} triangular space and close to the left margin. Photochemical aging led to increase in f_{44} for all the experiments, suggesting transformation of OA from SV-OOA to LV-OOA. For comparison, the f_{43} did not change significantly in all the experiments. The main ions at m/z 43 were $C_2H_3O^+$ and $C_3H_7^+$. It can be observed in Figure 6c that the increased contribution of $C_2H_3O^+$ and the decrease contribution of $C_3H_7^+$ were comparable during photoreaction.

The ion at m/z 60, mainly consisting of $C_2H_4O_2^+$, is regarded as a BBOA marker, and the mass fraction of this ion in OA, f_{60}, is widely used to probe the evolution of BBOA (Brito et al., 2014; May et al., 2015). Figure 7b plots evolution of f_{44} and f_{60} in all the experiments conducted in this study, in order to compare with measurements in aging biomass burning

plumes (Cubison et al., 2011) and those in the POA from different types of biomass burning (Alfarra et al., 2007; Brito et al., 2014; May et al., 2015). Photo-oxidation caused increase in f_{44} and decrease in f_{60}, and this is consistent with the general evolution of OA in ambient biomass burning plumes (Cubison et al., 2011). However, our measured f_{60}, 0.003-0.006 in the POA from open straw burning and 0.002-0004 in aged OA, were all lower than those from other field campaigns and quite near the background f_{60} level of 0.003 for ambient OA (Cubison et al., 2011; Figure 7b). Low values of f_{60} (0.005-0.02) were also reported by Hennigan et al. (2011) in a chamber study for fuels commonly burned in wildfires. In their study, biomass burning took place in a 3000 m^3 combustion chamber, and the smokes were then injected into another chamber for aging experiments with a dilution ratio of ~25. Previous studies have demonstrated that levoglucosan is a semi-volatile compound with a saturation concentration of ~8 μg m^{-3} at 293 K (Grieshop et al., 2009b; Huffman et al., 2009; Hennigan et al. 2011). As a result, high dilution conditions used in our study would cause levoglucosan to evaporate, and this may at least partly explain the low f_{60} observed in the POA from straw burning. From previous studies, the levoglucosan/OC ratios of straw burning ranging from 4.92 to 16.8% (4 types of vegetation summarized; Dhammapala et al., 2007; Kim Oanh et al., 2011; Hall et al., 2012) were not significantly (two-sample t-test, p>0.05) lower than those of prescribed fuel burning, wildfire and wood burning ranging from 1.46 to 13.5% (20 types of vegetation summarized; Hosseini et al., 2013; Shahid et al., 2015). So the difference in fuel type cannot explain the lower f_{60} observed in our study.

3.3.4 Elemental ratio and oxidation state of OA

In this study, the O/C and H/C ratios in the POA from different straws burning were in the range of 0.20-0.38 and 1.58-1.74, respectively. After 5 h aging, O/C increased and H/C decreased (Table 2). Kroll et al. (2011) proposed a metric, the average carbon oxidation state (OS_c), to describe the degree of oxidation of atmospheric organic species. OS_c could be

calculated from the elemental composition of OA measured by AMS, given by Eq. (7):

$$OS_c = 2 \times O/C - O/H \quad (7)$$

In this study, the OS_c values for the fresh POA from open straw burning ranged from -1.25 to -0.89, consistent with those suggested for BBOA (-1 to -0.7) (Kroll et al. 2011). During photochemical aging, the OS_c values increased linearly (p<0.001) with OH exposure (Figure 8), and the slopes were quite near each other even for different types of straws, implying AMS measured OS_c might be a good indicator of OH exposure and thereby of photochemical aging.

Figure 9 shows the Van Krevelen diagram of OA. In this study, the slopes of linear correlations between H/C and O/C range from -0.49 to -0.24 for the five experiments. Slopes of -1, 0.5 and 0 in the Van Krevelen diagrams indicate addition of carboxylic acids without fragmentation, addition of carboxylic acids with fragmentation, and addition of alcohols/peroxides, respectively (Heald et al., 2010; Ng et al., 2011a). Therefore, the slopes determined in our study suggest that open straw burning OA aging resulted in net changes in chemical composition equivalent to addition of carboxylic acid groups with C-C bond breakage and addition of alcohol/peroxide functional groups.

4 Conclusion

In this study, primary emissions of open burning of rice, corn and wheat straw and their photochemical were investigated using a large indoor chamber. Emission factors of NO_x, NH_3, SO_2, 67 NMHCs, PM and particle number were measured under dilution ratios ranging from 1300 to 4000. Emission factors of PM (3.73 to 6.36 g kg^{-1}) and POC (2.05 to 4.11 gC kg^{-1}) were lower than those reported in previous studies conducted at lower dilution ratios, probably due to the evaporation of semi-volatile organic compounds. Emission factors of POC, PM and major NMHCs compounds were all negatively correlated with the modified combustion efficiency, suggesting that incomplete burning of agricultural residues could lead to larger primary emission. Photochemical aging of primary emissions was investigated with OH

490 exposure equal to 3.2-9.2 hours under typical ambient conditions, and at the end of experiments
491 the OA mass concentrations increased by a factor of 2.4-7.6, suggesting that SOA could be
492 rapidly produced within several hours. Our estimation suggests that phenols are the most
493 important identified SOA precursors, and more than 70% of the formed OA still cannot be
494 explained by the oxidation of known precursors. Measurements using HR-TOF-AMS reveal
495 that after photochemical aging, signals for oxygen- and nitrogen-containing compounds were
496 largely increased, with OS_c increased in a highly significant linear way with OH exposure.
497

498 **Acknowledgements**

499 This study was supported by Strategic Priority Research Program of the Chinese Academy of
500 Sciences (Grant No. XDB05010200), National Natural Science Foundation of China (Grant
501 No. 41530641/41571130031/41673116), National Key Research and Development Program
502 (2016YFC0202204) and Guangzhou Science Technology and Innovation Commission
503 (201505231532347).
504

505 **References**

506 Adler, G., Flores, J. M., Riziq, A. A., Borrmann, S., and Rudich, Y.: Chemical, physical, and
507 optical evolution of biomass burning aerosols: a case study, Atmos. Chem. Phys., 11,
508 1491-1503, doi:10.5194/acp-11-1491-2011, 2011.
509 Aiken, A. C., DeCarlo, P. F., and Jimenez, J. L.: Elemental analysis of organic species with
510 electron ionization high-resolution mass spectrometry, Anal. Chem., 79, 8350-8358,
511 doi:10.1021/ac071150w, 2007.
512 Aiken, A. C., Decarlo, P. F., Kroll, J. H., Worsnop, D. R., Huffman, J. A., Docherty, K. S.,
513 Ulbrich, I. M., Mohr, C., Kimmel, J. R., Sueper, D., Sun, Y., Zhang, Q., Trimborn, A.,
514 Northway, M., Ziemann, P. J., Canagaratna, M. R., Onasch, T. B., Alfarra, M. R., Prevot,

A. S. H., Dommen, J., Duplissy, J., Metzger, A., Baltensperger, U., and Jimenez, J. L.: O/C and OM/OC ratios of primary, secondary, and ambient organic aerosols with high-resolution time-of-flight aerosol mass spectrometry, Environ. Sci. Technol., 42, 4478-4485, doi:10.1021/es703009q, 2008.

Akagi, S. K., Yokelson, R. J., Wiedinmyer, C., Alvarado, M. J., Reid, J. S., Karl, T., Crounse, J. D., and Wennberg, P. O.: Emission factors for open and domestic biomass burning for use in atmospheric models, Atmos. Chem. Phys., 11, 4039-4072, doi:10.5194/acp-11-4039-2011, 2011.

Alfarra, M. R., Prevot, A. S. H., Szidat, S., Sandradewi, J., Weimer, S., Lanz, V. A., Schreiber, D., Mohr, M., and Baltensperger, U.: Identification of the mass spectral signature of organic aerosols from wood burning emissions, Environ. Sci. Technol., 41, 5770-5777, doi:10.1021/es062289b, 2007.

Alves, N. d. O., Brito, J., Caumo, S., Arana, A., Hacon, S. d. S., Artaxo, P., Hillamo, R., Teinila, K., Batistuzzo de Medeiros, S. R., and Vasconcellos, P. d. C.: Biomass burning in the Amazon region: Aerosol source apportionment and associated health risk assessment, Atmos. Environ., 120, 277-285, doi:10.1016/j.atmosenv.2015.08.059, 2015.

Andreae, M. O., and Merlet, P.: Emission of trace gases and aerosols from biomass burning, Global Biogeochem. Cy., 15, 955-966, doi:10.1029/2000GB001382, 2001.

Andreae, M. O., Rosenfeld, D., Artaxo, P., Costa, A. A., Frank, G. P., Longo, K. M., and Silva-Dias, M. A. F.: Smoking Rain Clouds over the Amazon, Science, 303, 1337-1342, doi:10.1126/science.1092779, 2004.

Arnold, S. R., Emmons, L. K., Monks, S. A., Law, K. S., Ridley, D. A., Turquety, S., Tilmes, S., Thomas, J. L., Bouarar, I., Flemming, J., Huijnen, V., Mao, J., Duncan, B. N., Steenrod, S., Yoshida, Y., Langner, J., and Long, Y.: Biomass burning influence on high-latitude tropospheric ozone and reactive nitrogen in summer 2008: a multi-model analysis based

on POLMIP simulations, Atmos. Chem. Phys., 15, 6047-6068, doi:10.5194/acp-15-6047-2015, 2015.

Betha, R., Zhang, Z., and Balasubramanian, R.: Influence of trans-boundary biomass burning impacted air masses on submicron particle number concentrations and size distributions, Atmos. Environ., 92, 9-18, doi:10.1016/j.atmosenv.2014.04.002, 2014.

Bond, T. C., Streets, D. G., Yarber, K. F., Nelson, S. M., Woo, J. H., and Klimont, Z.: A technology-based global inventory of black and organic carbon emissions from combustion, J. Geophys. Res.-Atmos., 109, 43, doi:10.1029/2003jd003697, 2004.

Borras, E., and Tortajada-Genaro, L. A.: Secondary organic aerosol formation from the photo-oxidation of benzene, Atmos. Environ., 47, 154-163, doi:10.1016/j.atmosenv.2011.11.020, 2012.

Brassard, P., Palacios, J. H., Godbout, S., Bussieres, D., Lagace, R., Larouche, J. P., and Pelletier, F.: Comparison of the gaseous and particulate matter emissions from the combustion of agricultural and forest biomasses, Bioresour. Technol., 155, 300-306, doi:10.1016/j.biortech.2013.12.027, 2014.

Brito, J., Rizzo, L. V., Morgan, W. T., Coe, H., Johnson, B., Haywood, J., Longo, K., Freitas, S., Andreae, M. O., and Artaxo, P.: Ground-based aerosol characterization during the South American Biomass Burning Analysis (SAMBBA) field experiment, Atmos. Chem. Phys., 14, 12069-12083, doi:10.5194/acp-14-12069-2014, 2014.

Bruns, E. A., El Haddad, I., Slowik, J. G., Kilic, D., Klein, F., Baltensperger, U., and Prevot, A. S. H.: Identification of significant precursor gases of secondary organic aerosols from residential wood combustion, Sci. Rep., 6, doi:10.1038/srep27881, 2016.

Canagaratna, M. R., Jimenez, J. L., Kroll, J. H., Chen, Q., Kessler, S. H., Massoli, P., Hildebrandt Ruiz, L., Fortner, E., Williams, L. R., Wilson, K. R., Surratt, J. D., Donahue, N. M., Jayne, J. T., and Worsnop, D. R.: Elemental ratio measurements of organic

compounds using aerosol mass spectrometry: characterization, improved calibration, and implications, Atmos. Chem. Phys., 15, 253-272, doi:10.5194/acp-15-253-2015, 2015.

Cao, G., Zhang, X., Gong, S., and Zheng, F.: Investigation on emission factors of particulate matter and gaseous pollutants from crop residue burning, J. Environ. Sci., 20, 50-55, doi:10.1016/S1001-0742(08)60007-8, 2008.

Carter, W. P. L.: Reactivity estimates for selected comsumer product compounds., Air resources Board, Califonia, Contract No. 06-408, 72-99, 2008.

Chan, A. W. H., Kautzman, K. E., Chhabra, P. S., Surratt, J. D., Chan, M. N., Crounse, J. D., Kürten, A., Wennberg, P. O., Flagan, R. C., and Seinfeld, J. H.: Secondary organic aerosol formation from photooxidation of naphthalene and alkylnaphthalenes: implications for oxidation of intermediate volatility organic compounds (IVOCs), Atmos. Chem. Phys., 9, 3049-3060, doi:10.5194/acp-9-3049-2009, 2009.

Chan, A. W. H., Chan, M. N., Surratt, J. D., and Chhabra, P. S.: Role of aldehyde chemistry and NO_x concentrations in secondary organic aerosol formation, Atmos. Chem. Phys., 10, 7169-7188, doi:10.5194/acp-10-7169-2010, 2010.

Cheng, Y., Engling, G., He, K. B., Duan, F. K., Ma, Y. L., Du, Z. Y., Liu, J. M., Zheng, M., and Weber, R. J.: Biomass burning contribution to Beijing aerosol, Atmos. Chem. Phys., 13, 7765-7781, doi:10.5194/acp-13-7765-2013, 2013.

Cheng, Y., Engling, G., Moosmaller, H., Arnott, W. P., Chen, L. W. A., Wold, C. E., Hao, W. M., and He, K. B.: Light absorption by biomass burning source emissions, Atmos. Environ., 127, 347-354, doi:10.1016/j.atmosenv.2015.12.045, 2016.

Chhabra, P. S., Ng, N. L., Canagaratna, M. R., Corrigan, A. L., Russell, L. M., Worsnop, D. R., Flagan, R. C., and Seinfeld, J. H.: Elemental composition and oxidation of chamber organic aerosol, Atmos. Chem. Phys., 11, 8827-8845, doi:10.5194/acp-11-8827-2011, 2011.

590 Christian, T. J., Yokelson, R. J., Cardenas, B., Molina, L. T., Engling, G., and Hsu, S. C.: Trace
591 gas and particle emissions from domestic and industrial biofuel use and garbage burning
592 in central Mexico, Atmos. Chem. Phys., 10, 565-584, doi:10.5194/acp-10-565-2010, 2010.
593 Cubison, M. J., Ortega, A. M., Hayes, P. L., Farmer, D. K., Day, D., Lechner, M. J., Brune, W.
594 H., Apel, E., Diskin, G. S., Fisher, J. A., Fuelberg, H. E., Hecobian, A., Knapp, D. J.,
595 Mikoviny, T., Riemer, D., Sachse, G. W., Sessions, W., Weber, R. J., Weinheimer, A. J.,
596 Wisthaler, A., and Jimenez, J. L.: Effects of aging on organic aerosol from open biomass
597 burning smoke in aircraft and laboratory studies, Atmos. Chem. Phys., 11, 12049-12064,
598 doi:10.5194/acp-11-12049-2011, 2011.
599 DeCarlo, P. F., Slowik, J. G., Worsnop, D. R., Davidovits, P., and Jimenez, J. L.: Particle
600 morphology and density characterization by combined mobility and aerodynamic
601 diameter measurements. Part 1: Theory, Aerosol Sci. Technol., 38, 1185-1205,
602 doi:10.1080/027868290903907, 2004.
603 DeCarlo, P. F., Kimmel, J. R., Trimborn, A., Northway, M. J., Jayne, J. T., Aiken, A. C., Gonin,
604 M., Fuhrer, K., Horvath, T., Docherty, K. S., Worsnop, D. R., and Jimenez, J. L.: Field-
605 deployable, high-resolution, time-of-flight aerosol mass spectrometer, Anal. Chem., 78,
606 8281-8289, doi:10.1021/ac061249n, 2006.
607 Dhammapala, R., Claiborn, C., Jimenez, J., Corkill, J., Gullett, B., Simpson, C., and Paulsen,
608 M.: Emission factors of PAHs, methoxyphenols, levoglucosan, elemental carbon and
609 organic carbon from simulated wheat and Kentucky bluegrass stubble burns, Atmos.
610 Environ., 41, 2660-2669, doi:10.1016/j.atmosenv.2006.11.023, 2007.
611 Ding, X., He, Q.-F., Shen, R.-Q., Yu, Q.-Q., Zhang, Y.-Q., Xin, J.-Y., Wen, T.-X., and Wang,
612 X.-M.: Spatial and seasonal variations of isoprene secondary organic aerosol in China:
613 Significant impact of biomass burning during winter, Sci. Rep., 6, 20411,
614 doi:10.1038/srep20411, 2016a.

615 Ding, X., Zhang, Y.-Q., He, Q.-F., Yu, Q.-Q., Shen, R.-Q., Zhang, Y., Zhang, Z., Lyu, S.-J., Hu,
616 Q.-H., Wang, Y.-S., Li, L.-F., Song, W., and Wang, X.-M.: Spatial and seasonal variations
617 of secondary organic aerosol from terpenoids over China, J. Geophys. Res.-Atmos., 121,
618 14661–14678, doi:10.1002/2016JD025467, 2016b.
619 Ding, X., Zhang, Y.-Q., He, Q.-F., Yu, Q.-Q., Wang, J.-Q., Shen, R.-Q., Song, W., Wang, Y.-S.,
620 and Wang, X.-M.: Significant increase of aromatics-derived secondary organic aerosol
621 during fall to winter in China, Environ. Sci. Technol., doi:10.1021/acs.est.6b06408, 2017.
622 Duncan, B. N., Bey, I., Chin, M., Mickley, L. J., Fairlie, T. D., Martin, R. V., and Matsueda, H.:
623 Indonesian wildfires of 1997: Impact on tropospheric chemistry, J. Geophys. Res.-Atmos.,
624 108, 25, doi:10.1029/2002jd003195, 2003.
625 Ervens, B., Turpin, B. J., and Weber, R. J.: Secondary organic aerosol formation in cloud
626 droplets and aqueous particles (aqSOA): a review of laboratory, field and model studies,
627 Atmos. Chem. Phys., 11, 11069-11102, doi:10.5194/acp-11-11069-2011, 2011.
628 Food and Agriculture Organization of the United Nation: Emissions of methane and nitrous
629 oxide from the on-site combustion of crop residues,
630 http://faostat3.fao.org/browse/G1/GB/E, last accessed: 6 April 2017.
631 Ge, S., Xu, X., Chow, J. C., Watson, J., Sheng, Q., Liu, W. L., Bai, Z. P., Zhu, T., Zhang, J. F.:
632 Emissions of air pollutants from household stoves: Honeycomb coal versus coal
633 cake, Environ. Sci. Technol., 38, 4612-4618, doi:10.1021/es049942k, 2004.
634 Ge, S., Xu, Y., and Jia, L.: Secondary organic aerosol formation from ethyne in the presence of
635 NaCl in a smog chamber, Environ. Chem., 13, 699-710, doi:10.1071/en15155, 2016.
636 Ge, S., Xu, Y., and Jia, L.: Secondary organic aerosol formation from propylene irradiations in
637 a chamber study, Atmos. Environ., 157, 146-155, doi:10.1016/j.atmosenv.2017.03.019,
638 2017.
639 Giordano, M. R., Short, D. Z., Hosseini, S., Lichtenberg, W., and Asa-Awuku, A. A.: Changes

in droplet surface tension affect the observed hygroscopicity of photochemically aged biomass burning aerosol, Environ. Sci. Technol., 47, 10980-10986, doi:10.1021/es401867j, 2013.

Gómez Alvarez, E., Borras, E., Viidanoja, J., and Hjorth, J.: Unsaturated dicarbonyl products from the OH-initiated photo-oxidation of furan, 2-methylfuran and 3-methylfuran, Atmos. Environ., 43, 1603-1612, doi:10.1016/j.atmosenv.2008.12.019, 2009.

Grieshop, A. P., Donahue, N. M., and Robinson, A. L.: Laboratory investigation of photochemical oxidation of organic aerosol from wood fires 2: analysis of aerosol mass spectrometer data, Atmos. Chem. Phys., 9, 2227-2240, doi:10.5194/acp-9-2227-2009, 2009a.

Grieshop, A. P., Logue, J. M., Donahue, N. M., and Robinson, A. L.: Laboratory investigation of photochemical oxidation of organic aerosol from wood fires 1: measurement and simulation of organic aerosol evolution, Atmos. Chem. Phys., 9, 1263-1277, doi:10.5194/acp-9-1263-2009, 2009b.

Hall, D., Wu, C. Y., Hsu, Y. M., Stormer, J., Engling, G., Capeto, K., Wang, J., Brown, S., Li, H. W., and Yu, K. M.: PAHs, carbonyls, VOCs and $PM_{2.5}$ emission factors for pre-harvest burning of Florida sugarcane, Atmos. Environ., 55, 164-172, doi:10.1016/j.atmosenv.2012.03.034, 2012.

Hayes, P. L., Ortega, A. M., Cubison, M. J., Froyd, K. D., Zhao, Y., Cliff, S. S., Hu, W. W., Toohey, D. W., Flynn, J. H., Lefer, B. L., Grossberg, N., Alvarez, S., Rappenglueck, B., Taylor, J. W., Allan, J. D., Holloway, J. S., Gilman, J. B., Kuster, W. C., De Gouw, J. A., Massoli, P., Zhang, X., Liu, J., Weber, R. J., Corrigan, A. L., Russell, L. M., Isaacman, G., Worton, D. R., Kreisberg, N. M., Goldstein, A. H., Thalman, R., Waxman, E. M., Volkamer, R., Lin, Y. H., Surratt, J. D., Kleindienst, T. E., Offenberg, J. H., Dusanter, S., Griffith, S., Stevens, P. S., Brioude, J., Angevine, W. M., and Jimenez, J. L.: Organic

665 aerosol composition and sources in Pasadena, California, during the 2010 CalNex
666 campaign, J. Geophys. Res.-Atmos., 118, 9233-9257, doi:10.1002/jgrd.50530, 2013.
667 Heald, C. L., Kroll, J. H., Jimenez, J. L., Docherty, K. S., DeCarlo, P. F., Aiken, A. C., Chen,
668 Q., Martin, S. T., Farmer, D. K., and Artaxo, P.: A simplified description of the evolution
669 of organic aerosol composition in the atmosphere, Geophys. Res. Lett., 37, L08803,
670 doi:10.1029/2010gl042737, 2010.
671 Hennigan, C. J., Miracolo, M. A., Engelhart, G. J., May, A. A., Presto, A. A., Lee, T., Sullivan,
672 A. P., McMeeking, G. R., Coe, H., Wold, C. E., Hao, W. M., Gilman, J. B., Kuster, W. C.,
673 de Gouw, J., Schichtel, B. A., Collett, J. L., Kreidenweis, S. M., and Robinson, A. L.:
674 Chemical and physical transformations of organic aerosol from the photo-oxidation of
675 open biomass burning emissions in an environmental chamber, Atmos. Chem. Phys., 11,
676 7669-7686, doi:10.5194/acp-11-7669-2011, 2011.
677 Henry, K. M., Lohaus, T., and Donahue, N. M.: Organic aerosol yields from α-pinene oxidation:
678 bridging the gap between first-generation yields and aging chemistry, Environ. Sci.
679 Technol., 46, 12347-12354, doi:10.1021/es302060y, 2012.
680 Heringa, M. F., DeCarlo, P. F., Chirico, R., Tritscher, T., Dommen, J., Weingartner, E., Richter,
681 R., Wehrle, G., Prévôt, A. S. H., and Baltensperger, U.: Investigations of primary and
682 secondary particulate matter of different wood combustion appliances with a high-
683 resolution time-of-flight aerosol mass spectrometer, Atmos. Chem. Phys., 11, 5945-5957,
684 doi:10.5194/acp-11-5945-2011, 2011.
685 Hildebrandt, L., Donahue, N. M., and Pandis, S. N.: High formation of secondary organic
686 aerosol from the photo-oxidation of toluene, Atmos. Chem. Phys., 9, 2973-2986,
687 doi:10.5194/acp-9-2973-2009, 2009.
688 Hossain, A., Park, S., Kim, J. S., and Park, K.: Volatility and mixing states of ultrafine particles
689 from biomass burning, J. Hazard. Mater., 205, 189-197,

690 doi:10.1016/j.jhazmat.2011.12.061, 2012.
691 Hosseini, S., Urbanski, S. P., Dixit, P., Qi, L., Burling, I. R., Yokelson, R. J., Johnson, T. J.,
692 Shrivastava, M., Jung, H. S., Weise, D. R., Miller, J. W., and Cocker, D. R.: Laboratory
693 characterization of PM emissions from combustion of wildland biomass fuels, J. Geophys.
694 Res.-Atmos., 118, 9914-9929, doi:10.1002/jgrd.50481, 2013.
695 Huang, R. J., Zhang, Y. L., Bozzetti, C., Ho, K. F., Cao, J. J., Han, Y. M., Daellenbach, K. R.,
696 Slowik, J. G., Platt, S. M., Canonaco, F., Zotter, P., Wolf, R., Pieber, S. M., Bruns, E. A.,
697 Crippa, M., Ciarelli, G., Piazzalunga, A., Schwikowski, M., Abbaszade, G., Schnelle-
698 Kreis, J., Zimmermann, R., An, Z. S., Szidat, S., Baltensperger, U., El Haddad, I., and
699 Prevot, A. S. H.: High secondary aerosol contribution to particulate pollution during haze
700 events in China, Nature, 514, 218-222, doi:10.1038/nature13774, 2014.
701 Huang, X., Ding, A., Liu, L., Liu, Q., Ding, K., Niu, X., Nie, W., Xu, Z., Chi, X., Wang, M.,
702 Sun, J., Guo, W., and Fu, C.: Effects of aerosol-radiation interaction on precipitation
703 during biomass-burning season in East China, Atmos. Chem. Phys., 16, 10063-10082,
704 doi:10.5194/acp-16-10063-2016, 2016.
705 Huang, Y., Shen, H. Z., Chen, Y. L., Zhong, Q. R., Chen, H., Wang, R., Shen, G. F., Liu, J. F.,
706 Li, B. G., and Tao, S.: Global organic carbon emissions from primary sources from 1960
707 to 2009, Atmos. Environ., 122, 505-512, doi:10.1016/j.atmosenv.2015.10.017, 2015.
708 Huang, Z., Zhang, Y., Yan, Q., Zhang, Z., and Wang, X.: Real-time monitoring of respiratory
709 absorption factors of volatile organic compounds in ambient air by proton transfer reaction
710 time-of-flight mass spectrometry, J. Hazard. Mater., 320, 547-555,
711 doi:10.1016/j.jhazmat.2016.08.064, 2016.
712 Huffman, J. A., Docherty, K. S., Mohr, C., Cubison, M. J., Ulbrich, I. M., Ziemann, P. J.,
713 Onasch, T. B., and Jimenez, J. L.: Chemically-resolved volatility measurements of organic
714 aerosol from different sources, Environ. Sci. Technol., 43, 5351-5357,

715 doi:10.1021/es803539d, 2009.
716 Jathar, S. H., Gordon, T. D., Hennigan, C. J., Pye, H. O. T., Pouliot, G., Adams, P. J., Donahue,
717 N. M., and Robinson, A. L.: Unspeciated organic emissions from combustion sources and
718 their influence on the secondary organic aerosol budget in the United States, Proc. Natl.
719 Acad. Sci. U. S. A., 111, 10473-10478, doi:10.1073/pnas.1323740111, 2014.
720 Jia, L., and Xu, Y.: Ozone and secondary organic aerosol formation from Ethylene-NO_x-NaCl
721 irradiations under different relative humidity conditions, J. Atmos. Chem., 73, 81-100,
722 doi:10.1007/s10874-015-9317-1, 2016.
723 Jolleys, M. D., Coe, H., McFiggans, G., Capes, G., Allan, J. D., Crosier, J., Williams, P. I.,
724 Allen, G., Bower, K. N., Jimenez, J. L., Russell, L. M., Grutter, M., and Baumgardner, D.:
725 Characterizing the aging of biomass burning organic aerosol by use of mixing ratios: a
726 meta-analysis of four regions, Environ. Sci. Technol., 46, 13093-13102,
727 doi:10.1021/es302386v, 2012.
728 Kim Oanh, N. T., Ly, B. T., Tipayarom, D., Manandhar, B. R., Prapat, P., Simpson, C. D., and
729 Sally Liu, L. J.: Characterization of particulate matter emission from open burning of rice
730 straw, Atmos. Environ., 45, 493-502, doi:10.1016/j.atmosenv.2010.09.023, 2011.
731 Kim Oanh, N. T., Tipayarom, A., Bich, T. L., Tipayarom, D., Simpson, C. D., Hardie, D., and
732 Sally Liu, L. J.: Characterization of gaseous and semi-volatile organic compounds emitted
733 from field burning of rice straw, Atmos. Environ., 119, 182-191,
734 doi:10.1016/j.atmosenv.2015.08.005, 2015.
735 Kirchstetter, T. W., and Novakov, T.: Controlled generation of black carbon particles from a
736 diffusion flame and applications in evaluating black carbon measurement methods, Atmos.
737 Environ., 41, 1874-1888, doi:10.1016/j.atmosenv.2006.10.067, 2007.
738 Koren, I., Kaufman, Y. J., Remer, L. A., and Martins, J. V.: Measurement of the effect of
739 Amazon smoke on inhibition of cloud formation, Science, 303, 1342-1345,

740 doi:10.1126/science.1089424, 2004.
741 Kroll, J. H., Donahue, N. M., Jimenez, J. L., Kessler, S. H., Canagaratna, M. R., Wilson, K. R.,
742 Altieri, K. E., Mazzoleni, L. R., Wozniak, A. S., and Bluhm, H.: Carbon oxidation state
743 as a metric for describing the chemistry of atmospheric organic aerosol, Nat. Chem., 3,
744 133-139, doi:10.1038/nchem.948, 2011.
745 Lambe, A. T., Ahern, A. T., Williams, L. R., Slowik, J. G., Wong, J. P. S., Abbatt, J. P. D.,
746 Brune, W. H., Ng, N. L., Wright, J. P., Croasdale, D. R., Worsnop, D. R., Davidovits, P.,
747 and Onasch, T. B.: Characterization of aerosol photooxidation flow reactors:
748 heterogeneous oxidation, secondary organic aerosol formation and cloud condensation
749 nuclei activity measurements, Atmos. Meas. Tech., 4, 445-461, doi:10.5194/amt-4-445-
750 2011, 2011.
751 Laskin, A., Laskin, J., and Nizkorodov, S. A.: Chemistry of atmospheric brown carbon, Chem.
752 Rev., 115, 4335-4382, doi:10.1021/cr5006167, 2015.
753 Li, C., Ma, Z., Chen, J., Wang, X., Ye, X., Wang, L., Yang, X., Kan, H., Donaldson, D. J., and
754 Mellouki, A.: Evolution of biomass burning smoke particles in the dark, Atmos. Environ.,
755 120, 244-252, doi:10.1016/j.atmosenv.2015.09.003, 2015.
756 Li, C., Hu, Y., Zhang, F., Chen, J., Ma, Z., Ye, X., Yang, X., Wang, L., Tang, X., Zhang, R., Mu,
757 M., Wang, G., Kan, H., Wang, X., and Mellouki, A.: Multi-pollutant emissions from the
758 burning of major agricultural residues in China and the related health-economic effects,
759 Atmos. Chem. Phys., 17, 4957-4988, doi:10.5194/acp-17-4957-2017, 2017.
760 Li, J., Bo, Y., and Xie, S. D.: Estimating emissions from crop residue open burning in China
761 based on statistics and MODIS fire products, J. Environ. Sci., 44, 158-170,
762 doi:10.1016/j.jes.2015.08.024, 2016.
763 Li, X. G., Wang, S. X., Duan, L., Hao, J., Li, C., Chen, Y. S., and Yang, L.: Particulate and trace
764 gas emissions from open burning of wheat straw and corn stover in China, Environ. Sci.

765 Technol., 41, 6052-6058, doi:10.1021/es0705137, 2007.
766 Li, X. H., Wang, S. X., Duan, L., and Hao, J. M.: Characterization of non-methane
767 hydrocarbons emitted from open burning of wheat straw and corn stover in China, Environ.
768 Res. Lett., 4, 7, doi:10.1088/1748-9326/4/4/044015, 2009.
769 Lim, Y. B., Tan, Y., and Turpin, B. J.: Chemical insights, explicit chemistry, and yields of
770 secondary organic aerosol from OH radical oxidation of methylglyoxal and glyoxal in the
771 aqueous phase, Atmos. Chem. Phys., 13, 8651-8667, doi:10.5194/acp-13-8651-2013,
772 2013.
773 Lipsky, E. M., and Robinson, A. L.: Effects of dilution on fine particle mass and partitioning
774 of semivolatile organics in diesel exhaust and wood smoke, Environ. Sci. Technol., 40,
775 155-162, doi:10.1021/es050319p, 2006.
776 Liu, T., Wang, X., Deng, W., Hu, Q., Ding, X., Zhang, Y., He, Q., Zhang, Z., Lu, S., Bi, X.,
777 Chen, J., and Yu, J.: Secondary organic aerosol formation from photochemical aging of
778 light-duty gasoline vehicle exhausts in a smog chamber, Atmos. Chem. Phys., 15, 9049-
779 9062, doi:10.5194/acp-15-9049-2015, 2015.
780 Liu, X. X., Zhang, Y., Huey, L. G., Yokelson, R. J., Wang, Y., Jimenez, J. L., Campuzano-Jost,
781 P., Beyersdorf, A. J., Blake, D. R., Choi, Y., St Clair, J. M., Crounse, J. D., Day, D. A.,
782 Diskin, G. S., Fried, A., Hall, S. R., Hanisco, T. F., King, L. E., Meinardi, S., Mikoviny,
783 T., Palm, B. B., Peischl, J., Perring, A. E., Pollack, I. B., Ryerson, T. B., Sachse, G.,
784 Schwarz, J. P., Simpson, I. J., Tanner, D. J., Thornhill, K. L., Ullmann, K., Weber, R. J.,
785 Wennberg, P. O., Wisthaler, A., Wolfe, G. M., and Ziemba, L. D.: Agricultural fires in the
786 southeastern US during SEAC^{4}RS: Emissions of trace gases and particles and evolution
787 of ozone, reactive nitrogen, and organic aerosol, J. Geophys. Res.-Atmos., 121, 7383-
788 7414, doi:10.1002/2016jd025040, 2016.
789 Martin, M., Tritscher, T., Juranyi, Z., Heringa, M. F., Sierau, B., Weingartner, E., Chirico, R.,

790 Gysel, M., Prevot, A. S. H., Baltensperger, U., and Lohmann, U.: Hygroscopic properties
791 of fresh and aged wood burning particles, J. Aerosol Sci., 56, 15-29,
792 doi:10.1016/j.jaerosci.2012.08.006, 2013.
793 May, A. A., Levin, E. J. T., Hennigan, C. J., Riipinen, I., Lee, T., Collett, J. L., Jr., Jimenez, J.
794 L., Kreidenweis, S. M., and Robinson, A. L.: Gas-particle partitioning of primary organic
795 aerosol emissions: 3. Biomass burning, J. Geophys. Res.-Atmos., 118, 11327-11338,
796 doi:10.1002/jgrd.50828, 2013.
797 May, A. A., Lee, T., McMeeking, G. R., Akagi, S., Sullivan, A. P., Urbanski, S., Yokelson, R.
798 J., and Kreidenweis, S. M.: Observations and analysis of organic aerosol evolution in some
799 prescribed fire smoke plumes, Atmos. Chem. Phys., 15, 6323-6335, doi:10.5194/acp-15-
800 6323-2015, 2015.
801 McMurry, P. H., and Grosjean, D.: Gas and aerosol wall losses in Teflon film smog chambers,
802 Environ. Sci. Technol., 19, 1176-1182, doi:10.1021/es00142a006, 1985.
803 Müller, M., Anderson, B. E., Beyersdorf, A. J., Crawford, J. H., Diskin, G. S., Eichler, P., Fried,
804 A., Keutsch, F. N., Mikoviny, T., Thornhill, K. L., Walega, J. G., Weinheimer, A. J., Yang,
805 M., Yokelson, R. J., and Wisthaler, A.: In situ measurements and modeling of reactive
806 trace gases in a small biomass burning plume, Atmos. Chem. Phys., 16, 3813-3824,
807 doi:10.5194/acp-16-3813-2016, 2016.
808 Nakao, S., Clark, C., Tang, P., Sato, K., and Iii, D. C.: Secondary organic aerosol formation
809 from phenolic compounds in the absence of NO_x, Atmos. Chem. Phys., 11, 2025-2055,
810 doi:10.5194/acp-11-10649-2011, 2011.
811 National bureau of statistics of people's republic of China.: The statistical communiqu on
812 national economy and social development in 2015,
813 http://www.stats.gov.cn/tjsj/zxfb/201602/t20160229_1323991.html, last accessed: 6
814 April 2017.

815 Ng, N. L., Chhabra, P. S., Chan, A. W. H., Surratt, J. D., Kroll, J. H., Kwan, A. J., McCabe, D.
816 C., Wennberg, P. O., Sorooshian, A., Murphy, S. M., Dalleska, N. F., Flagan, R. C., and
817 Seinfeld, J. H.: Effect of NO_x level on secondary organic aerosol (SOA) formation from
818 the photooxidation of terpenes, Atmos. Chem. Phys., 7, 5159-5174, doi:10.5194/acp-7-
819 5159-2007, 2007a.
820 Ng, N. L., Kroll, J. H., Chan, A. W. H., Chhabra, P. S., Flagan, R. C., and Seinfeld, J. H.:
821 Secondary organic aerosol formation from m-xylene, toluene, and benzene, Atmos. Chem.
822 Phys., 7, 3909-3922, doi:10.5194/acp-7-3909-2007, 2007b.
823 Ng, N. L., Canagaratna, M. R., Zhang, Q., Jimenez, J. L., Tian, J., Ulbrich, I. M., Kroll, J. H.,
824 Docherty, K. S., Chhabra, P. S., Bahreini, R., Murphy, S. M., Seinfeld, J. H., Hildebrandt,
825 L., Donahue, N. M., DeCarlo, P. F., Lanz, V. A., Prevot, A. S. H., Dinar, E., Rudich, Y.,
826 and Worsnop, D. R.: Organic aerosol components observed in Northern Hemispheric
827 datasets from Aerosol Mass Spectrometry, Atmos. Chem. Phys., 10, 4625-4641,
828 doi:10.5194/acp-10-4625-2010, 2010.
829 Ng, N. L., Canagaratna, M. R., Jimenez, J. L., Chhabra, P. S., Seinfeld, J. H., and Worsnop, D.
830 R.: Changes in organic aerosol composition with aging inferred from aerosol mass spectra,
831 Atmos. Chem. Phys., 11, 6465-6474, doi:10.5194/acp-11-6465-2011, 2011a.
832 Ng, N. L., Canagaratna, M. R., Jimenez, J. L., Zhang, Q., Ulbrich, I. M., and Worsnop, D. R.:
833 Real-Time Methods for estimating organic cComponent mass concentrations from aerosol
834 mass spectrometer data, Environ. Sci. Technol., 45, 910-916, doi:10.1021/es102951k,
835 2011b.
836 Ni, H. Y., Han, Y. M., Cao, J. J., Chen, L. W. A., Tian, J., Wang, X. L., Chow, J. C., Watson, J.
837 G., Wang, Q. Y., Wang, P., Li, H., and Huang, R. J.: Emission characteristics of
838 carbonaceous particles and trace gases from open burning of crop residues in China,
839 Atmos. Environ., 123, 399-406, doi:10.1016/j.atmosenv.2015.05.007, 2015.

840 Niu, H. Y., Cheng, W. J., Hu, W., and Pian, W.: Characteristics of individual particles in a severe
841 short-period haze episode induced by biomass burning in Beijing, Atmos. Pollut. Res., 7,
842 1072-1081, doi:10.1016/j.apr.2016.05.011, 2016.
843 Ortega, A. M., Day, D. A., Cubison, M. J., Brune, W. H., Bon, D., de Gouw, J. A., and Jimenez,
844 J. L.: Secondary organic aerosol formation and primary organic aerosol oxidation from
845 biomass-burning smoke in a flow reactor during FLAME-3, Atmos. Chem. Phys., 13,
846 11551-11571, doi:10.5194/acp-13-11551-2013, 2013.
847 Real, E., Law, K. S., Weinzierl, B., Fiebig, M., Petzold, A., Wild, O., Methven, J., Arnold, S.,
848 Stohl, A., Huntrieser, H., Roiger, A., Schlager, H., Stewart, D., Avery, M., Sachse, G.,
849 Browell, E., Ferrare, R., and Blake, D.: Processes influencing ozone levels in Alaskan
850 forest fire plumes during long-range transport over the North Atlantic, J. Geophys. Res.-
851 Atmos., 112, doi:10.1029/2006jd007576, 2007.
852 Robinson, A. L., Donahue, N. M., Shrivastava, M. K., Weitkamp, E. A., Sage, A. M., Grieshop,
853 A. P., Lane, T. E., Pierce, J. R., and Pandis, S. N.: Rethinking organic aerosols:
854 semivolatile emissions and photochemical aging, Science, 315, 1259-1262,
855 doi:10.1126/science.1133061, 2007.
856 Sanchis, E., Ferrer, M., Calvet, S., Coscolla, C., Yusa, V., and Cambra-Lopez, M.: Gaseous and
857 particulate emission profiles during controlled rice straw burning, Atmos. Environ., 98,
858 25-31, doi:10.1016/j.atmosenv.2014.07.062, 2014.
859 Schmid, O., Artaxo, P., Arnott, W. P., Chand, D., Gatti, L. V., Frank, G. P., Hoffer, A., Schnaiter,
860 M., and Andreae, M. O.: Spectral light absorption by ambient aerosols influenced by
861 biomass burning in the Amazon Basin. I: Comparison and field calibration of absorption
862 measurement techniques, Atmos. Chem. Phys., 6, 3443-3462, doi:10.5194/acp-6-3443-
863 2006, 2006.
864 Schmid, O., Karg, E., Hagen, D. E., Whitefield, P. D., and Ferron, G. A.: On the effective

density of non-spherical particles as derived from combined measurements of aerodynamic and mobility equivalent size, J. Aerosol Sci., 38, 431-443, doi:10.1016/j.jaerosci.2007.01.002, 2007.

Shahid, I., Kistler, M., Mukhtar, A., Cruz, C. R. S., Bauer, H., and Puxbaum, H.: Chemical composition of particles from traditional burning of Pakistani wood species, Atmos. Environ., 121, 35-41, doi:10.1016/j.atmosenv.2015.01.041, 2015.

Shakya, K. M., and Griffin, R. J.: Secondary organic aerosol from photooxidation of polycyclic aromatic hydrocarbons, Environ. Sci. Technol., 44, 8134-8139, doi:10.1021/es1019417, 2010.

Shrivastava, M., Easter, R. C., Liu, X. H., Zelenyuk, A., Singh, B., Zhang, K., Ma, P. L., Chand, D., Ghan, S., Jimenez, J. L., Zhang, Q., Fast, J., Rasch, P. J., and Tiitta, P.: Global transformation and fate of SOA: Implications of low-volatility SOA and gas-phase fragmentation reactions, J. Geophys. Res.-Atmos., 120, 4169-4195, doi:10.1002/2014jd022563, 2015.

Spracklen, D. V., Jimenez, J. L., Carslaw, K. S., Worsnop, D. R., Evans, M. J., Mann, G. W., Zhang, Q., Canagaratna, M. R., Allan, J., Coe, H., McFiggans, G., Rap, A., and Forster, P.: Aerosol mass spectrometer constraint on the global secondary organic aerosol budget, Atmos. Chem. Phys., 11, 12109-12136, doi:10.5194/acp-11-12109-2011, 2011.

Stockwell, C. E., Yokelson, R. J., Kreidenweis, S. M., Robinson, A. L., DeMott, P. J., Sullivan, R. C., Reardon, J., Ryan, K. C., Griffith, D. W. T., and Stevens, L.: Trace gas emissions from combustion of peat, crop residue, domestic biofuels, grasses, and other fuels: configuration and Fourier transform infrared (FTIR) component of the fourth Fire Lab at Missoula Experiment (FLAME-4), Atmos. Chem. Phys., 14, 9727-9754, doi:10.5194/acp-14-9727-2014, 2014.

Stockwell, C. E., Veres, P. R., Williams, J., and Yokelson, R. J.: Characterization of biomass

burning emissions from cooking fires, peat, crop residue, and other fuels with high-resolution proton-transfer-reaction time-of-flight mass spectrometry, Atmos. Chem. Phys., 15, 845-865, doi:10.5194/acp-15-845-2015, 2015.

Streets, D. G., Yarber, K. F., Woo, J. H., and Carmichael, G. R.: Biomass burning in Asia: Annual and seasonal estimates and atmospheric emissions, Global Biogeochem. Cy., 17, 20, doi:10.1029/2003gb002040, 2003.

Takekawa, H., Minoura, H., and Yamazaki, S.: Temperature dependence of secondary organic aerosol formation by photo-oxidation of hydrocarbons, Atmos. Environ., 37, 3413-3424, doi:10.1016/s1352-2310(03)00359-5, 2003.

Tariq, S., ul-Haq, Z., and Ali, M.: Satellite and ground-based remote sensing of aerosols during intense haze event of October 2013 over lahore, Pakistan, Asia-Pac. J. Atmos. Sci., 52, 25-33, doi:10.1007/s13143-015-0084-3, 2016.

Thompson, A. M., Witte, J. C., Hudson, R. D., Guo, H., Herman, J. R., and Fujiwara, M.: Tropical tropospheric ozone and biomass burning, Science, 291, 2128-2132, doi:10.1126/science.291.5511.2128, 2001.

Tian, H., Zhao, D., and Wang, Y.: Emission inventories of atmospheric pollutants discharged from biomass burning in China, Acta Sci. Circumst., 31, 349-357 in Chinese, 2011.

Tissari, J., Lyyranen, J., Hytonen, K., Sippula, O., Tapper, U., Frey, A., Saarnio, K., Pennanen, A. S., Hillamo, R., Salonen, R. O., Hirvonen, M. R., and Jokiniemi, J.: Fine particle and gaseous emissions from normal and smouldering wood combustion in a conventional masonry heater, Atmos. Environ., 42, 7862-7873, doi:10.1016/j.atmosenv.2008.07.019, 2008.

Tiitta, P., Leskinen, A., Hao, L., Yli-Pirila, P., Kortelainen, M., Grigonyte, J., Tissari, J., Lamberg, H., Hartikainen, A., Kuuspalo, K., Kortelainen, A.-M., Virtanen, A., Lehtinen, K. E. J., Komppula, M., Pieber, S., Prevot, A. S. H., Onasch, T. B., Worsnop, D. R., Czech,

915 H., Zimmermann, R., Jokiniemi, J., and Sippula, O.: Transformation of logwood
916 combustion emissions in a smog chamber: formation of secondary organic aerosol and
917 changes in the primary organic aerosol upon daytime and nighttime aging, Atmos. Chem.
918 Phys., 16, 13251-13269, doi:10.5194/acp-16-13251-2016, 2016.
919 Tsigaridis, K., Daskalakis, N., Kanakidou, M., Adams, P. J., Artaxo, P., Bahadur, R., Balkanski,
920 Y., Bauer, S. E., Bellouin, N., Benedetti, A., Bergman, T., Berntsen, T. K., Beukes, J. P.,
921 Bian, H., Carslaw, K. S., Chin, M., Curci, G., Diehl, T., Easter, R. C., Ghan, S. J., Gong,
922 S. L., Hodzic, A., Hoyle, C. R., Iversen, T., Jathar, S., Jimenez, J. L., Kaiser, J. W.,
923 Kirkevåg, A., Koch, D., Kokkola, H., Lee, Y. H., Lin, G., Liu, X., Luo, G., Ma, X., Mann,
924 G. W., Mihalopoulos, N., Morcrette, J. J., Müller, J. F., Myhre, G., Myriokefalitakis, S.,
925 Ng, N. L., O'Donnell, D., Penner, J. E., Pozzoli, L., Pringle, K. J., Russell, L. M., Schulz,
926 M., Sciare, J., Seland, Ø., Shindell, D. T., Sillman, S., Skeie, R. B., Spracklen, D.,
927 Stavrakou, T., Steenrod, S. D., Takemura, T., Tiitta, P., Tilmes, S., Tost, H., van Noije, T.,
928 van Zyl, P. G., von Salzen, K., Yu, F., Wang, Z., Wang, Z., Zaveri, R. A., Zhang, H., Zhang,
929 K., Zhang, Q., and Zhang, X.: The AeroCom evaluation and intercomparison of organic
930 aerosol in global models, Atmos. Chem. Phys., 14, 10845-10895, doi:10.5194/acp-14-
931 10845-2014, 2014.
932 Wang, H., Lou, S., Huang, C., Qiao, L., Tang, X., Chen, C., Zeng, L., Wang, Q., Zhou, M., Lu,
933 S., and Yu, X.: Source profiles of volatile organic compounds from biomass burning in
934 Yangtze River Delta, China, Aerosol Air Qual. Res., 14, 818-828,
935 doi:10.4209/aaqr.2013.05.0174, 2014.
936 Wang, X., and Wu, T.: Release of isoprene and monoterpenes during the aerobic decomposition
937 of orange wastes from laboratory incubation experiments, Environ. Sci. Technol., 42,
938 3265-3270, doi:10.1021/es702999j, 2008.
939 Wang, X., Liu, T., Bernard, F., Ding, X., Wen, S., Zhang, Y., Zhang, Z., He, Q., Lu, S., Chen,

940 J., Saunders, S., and Yu, J.: Design and characterization of a smog chamber for studying
941 gas-phase chemical mechanisms and aerosol formation, Atmos. Meas. Tech., 7, 301-313,
942 doi:10.5194/amt-7-301-2014, 2014.
943 Ward, D. E., Susott, R. A., Kauffman, J. B., Babbitt, R. E., Cummings, D. L., Dias, B., Holben,
944 B. N., Kaufman, Y. J., Rasmussen, R. A., and Setzer, A. W.: Smoke and fire characteristics
945 for cerrado and deforestation burns in Brazil: BASE-B Experiment, J. Geophys. Res.-
946 Atmos., 97, 14601-14619, doi:10.1029/92JD01218, 1992.
947 Weimer, S., Alfarra, M. R., Schreiber, D., Mohr, M., Prevot, A. S. H., and Baltensperger, U.:
948 Organic aerosol mass spectral signatures from wood-burning emissions: Influence of
949 burning conditions and wood type, J. Geophys. Res.-Atmos., 113,
950 doi:10.1029/2007jd009309, 2008.
951 Weitkamp, E. A., Sage, A. M., Pierce, J. R., Donahue, N. M., and Robinson, A. L.: Organic
952 aerosol formation from photochemical oxidation of diesel exhaust in a smog chamber,
953 Environ. Sci. Technol., 41, 6969-6975, doi:10.1021/es070193r, 2007.
954 Yee, L. D., Kautzman, K. E., Loza, C. L., Schilling, K. A., Coggon, M. M., Chhabra, P. S.,
955 Chan, M. N., Chan, A. W. H., Hersey, S. P., Crounse, J. D., Wennberg, P. O., Flagan, R.
956 C., and Seinfeld, J. H.: Secondary organic aerosol formation from biomass burning
957 intermediates: phenol and methoxyphenols, Atmos. Chem. Phys., 13, 8019-8043,
958 doi:10.5194/acp-13-8019-2013, 2013.
959 Yi, Z. G., Wang, X. M., Sheng, G. Y., Zhang, D. Q., Zhou, G. Y., and Fu, J. M.: Soil uptake of
960 carbonyl sulfide in subtropical forests with different successional stages in south China, J.
961 Geophys. Res.-Atmos., 112, 11, doi:10.1029/2006jd008048, 2007.
962 Yokelson, R. J., Christian, T. J., Karl, T. G., and Guenther, A.: The tropical forest and fire
963 emissions experiment: laboratory fire measurements and synthesis of campaign data,
964 Atmos. Chem. Phys., 8, 3509-3527, doi:10.5194/acp-8-3509-2008, 2008.

965 Yokelson, R. J., Burling, I. R., Urbanski, S. P., Atlas, E. L., Adachi, K., Buseck, P. R.,
966 Wiedinmyer, C., Akagi, S. K., Toohey, D. W., and Wold, C. E.: Trace gas and particle
967 emissions from open biomass burning in Mexico, Atmos. Chem. Phys., 11, 6787-6808,
968 doi:10.5194/acp-11-6787-2011, 2011.
969 Zhang, H., Ye, X., Cheng, T., Chen, J., Yang, X., Wang, L., and Zhang, R.: A laboratory study
970 of agricultural crop residue combustion in China: Emission factors and emission inventory,
971 Atmos. Environ., 42, 8432-8441, doi:10.1016/j.atmosenv.2008.08.015, 2008.
972 Zhang, H., Hu, D., Chen, J., Ye, X., Wang, S. X., Hao, J. M., Wang, L., Zhang, R., and An, Z.:
973 Particle size distribution and polycyclic aromatic hydrocarbons emissions from
974 agricultural crop residue burning, Environ. Sci. Technol., 45, 5477-5482,
975 doi:10.1021/es1037904, 2011.
976 Zhang, Q., Jimenez, J.L., Canagaratna, M.R., Ulbrich, I.M., Ng, N.L., Worsnop, D.R., Sun,
977 Y.L.: Understanding atmospheric organic aerosols via factor analysis of aerosol mass
978 spectrometry: a review, Anal. Bioanal. Chem., 401, 3045-3067, doi: 10.1007/s00216-011-
979 5355-y, 2011
980 Zhang, Y. L., Guo, H., Wang, X. M., Simpson, I. J., Barletta, B., Blake, D. R., Meinardi, S.,
981 Rowland, F. S., Cheng, H. R., Saunders, S. M., and Lam, S. H. M.: Emission patterns and
982 spatiotemporal variations of halocarbons in the Pearl River Delta region, southern China,
983 J. Geophys. Res.-Atmos., 115, 16, doi:10.1029/2009jd013726, 2010.
984 Zhang, Y. L., Wang, X. M., Blake, D. R., Li, L. F., Zhang, Z., Wang, S. Y., Guo, H., Lee, F. S.
985 C., Gao, B., Chan, L. Y., Wu, D., and Rowland, F. S.: Aromatic hydrocarbons as ozone
986 precursors before and after outbreak of the 2008 financial crisis in the Pearl River Delta
987 region, south China, J. Geophys. Res.-Atmos., 117, 16, doi:10.1029/2011jd017356, 2012.
988

Atmos. Chem. Phys. Discuss., https://doi.org/10.5194/acp-2017-626
Manuscript under review for journal Atmos. Chem. Phys.
Discussion started: 23 August 2017

Atmospheric Chemistry and Physics Discussions

989 **Table 1.** Primary emission factors measured for agricultural residues burning. All the units are
990 g kg^{-1}, except the unit for particle number (PN) is 10^{15} particle kg^{-1}. MCE: modified combustion
991 efficiency; NMHCs: non-methane hydrocarbons; POA: primary organic aerosol; POC primary
992 organic carbon; BC: black carbon.

	Rice		Corn		Wheat	
Species	This study (n=9)	Others	This study (n=6)	Others	This study (n=5)	Others
MCE	0.926±0.049		0.953±0.019		0.949±0.035	
CO_2	1262±81		1477±28		1423±60	
CO	63.5±41.4		46.1±19.2		48.6±33.0	
NO_x	1.47±0.61	3.51±0.38[a]	5.00±3.94	4.3±1.8[b]	3.08±0.93	3.3±1.7[b]; 2.27±0.04[a]
NH_3	0.45±0.15	0.95±0.65[a]; 4.10±1.24[c]	0.63±0.30	0.68±0.52[b]	0.22±0.19	0.37±0.14[b]; 0.21±0.14[a]
SO_2	0.07±0.07	0.18±0.31[d]; 0.37±0.27[e]; 1.27±0.35[a]	0.99±1.53	0.04±0.04[d]	0.72±0.34	0.04±0.04[d]; 0.73±0.15[a]
NMHCs	5.04±2.04	1.25[f]	2.47±2.11	1.59±0.43[g]	3.08±2.43	1.69±0.58[g]; 0.90[f]
PM	3.73±3.28	8.5±6.7[h]; 8.3±2.2[e]; 13.2±1.44[i]; 4.2[c]	5.44±3.43	12.2±5.4[h]; 11.7±1.0[b]; 5.36±0.55[i]	6.36±2.98	11.4±4.9[h]; 7.6±4.1[b]; 5.30±0.30[i]
PN	2.94±0.91	0.018±0.001[j]	7.29±4.17	0.017±0.001[j]	5.87±2.89	0.010±0.001[j]
POA	2.99±1.00		3.99±2.68		5.96±0.19	
POC	2.05±0.72	3.3±2.8[h]; 6.02±0.60[i]	2.52±1.66	6.3±3.6[h]; 3.9±1.7[b]; 2.06±0.34[i]	4.11±0.29	5.1±3.0[h]; 2.7±1.0[b]; 2.42±0.13[i]
BC	0.22±0.11	0.21±0.13[h]	0.24±0.09	0.28±0.09[h]; 0.35±0.10[b]	0.27±0.07	0.24±0.12[h]; 0.49±0.12[b]

993 [a] Stockwell et al., 2015; [b] Li et al., 2007, PM correspond to $PM_{2.5}$; [c] Christian et al., 2003; [d] Cao et al., 2008; [e] Kim
994 Oanh et al., 2015, PM correspond to $PM_{2.5}$; [f] Wang et al., 2014, 56 NMHCs species summarized; [g] Li et al., 2009,
995 52 NMHCs species summarized; [h] Ni et al., 2015, PM correspond to $PM_{2.5}$; [i] Li et al., 2017, PM correspond to
996 PM_1; [j] Zhang et al., 2008.
997

Atmos. Chem. Phys. Discuss., https://doi.org/10.5194/acp-2017-626
Manuscript under review for journal Atmos. Chem. Phys.
Discussion started: 23 August 2017

Atmospheric Chemistry and Physics Discussions

998 **Table 2.** Overview of important experimental conditions and key results in the photochemical
999 oxidation experiments. The unit for OH exposure is 10^{10} molecule cm^{-3} s. NA: data was not
1000 available because no data was recorded in the W-mode.

NO.	Straw type	Temp (°C)	RH (%)	OH exposure	POA			Aged OA			OA ER
					O/C	H/C	OS_c	O/C	H/C	OS_c	
Burn 1	Rice	25.0±0.4	48.9±1.4	3.80	NA	NA	NA	NA	NA	NA	2.7
Burn 2	Rice	25.1±0.4	55.0±2.3	4.97	0.25	1.74	-1.25	0.50	1.65	-0.65	7.6
Burn 3	Corn	25.5±0.4	53.0±2.9	4.16	0.38	1.66	-0.89	0.60	1.66	-0.46	3.6
Burn 4	Corn	26.1±0.4	48.4±2.2	4.16	0.30	1.58	-0.97	0.65	1.57	-0.26	4.6
Burn 5	Wheat	25.3±0.5	52.8±2.2	3.20	0.20	1.66	-1.25	0.50	1.56	-0.55	2.4
Burn 6	Wheat	25.2±0.4	55.1±2.7	1.87	0.26	1.71	-1.20	0.53	1.66	-0.61	6.6

1001
1002

1003

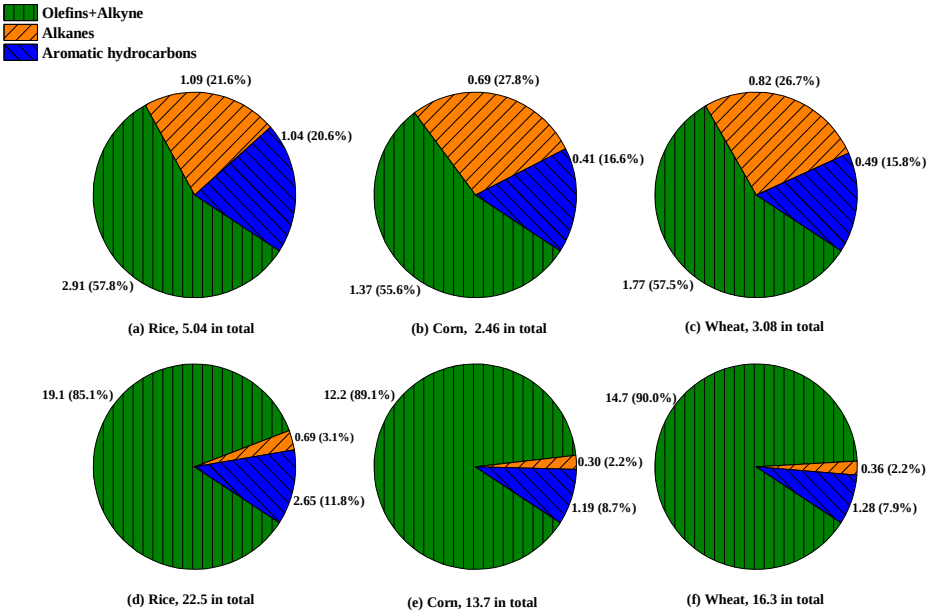

1004

1005 **Figure 1.** (a-c) Non-methane hydrocarbon (NMHC) compositions and (d-f) their relative

1006 contribution to ozone formation potential (OFP) for open burning of rice, corn and wheat straw.

1007

Atmos. Chem. Phys. Discuss., https://doi.org/10.5194/acp-2017-626
Manuscript under review for journal Atmos. Chem. Phys.
Discussion started: 23 August 2017

Atmospheric Chemistry and Physics Discussions

1008

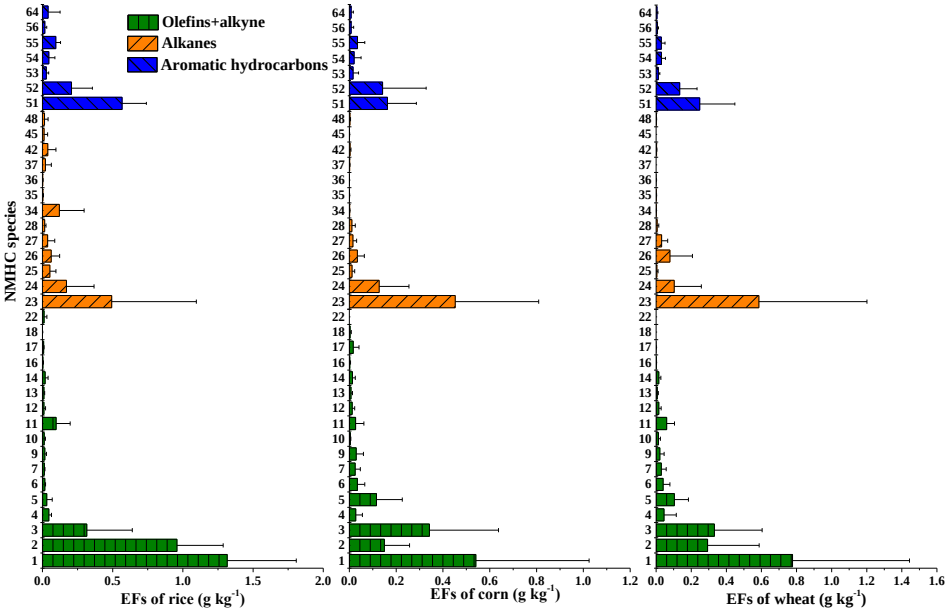

1009

1010 **Figure 2.** Emission factors (EFs) of NMHCs for straw burning of rice, corn and wheat. Only

1011 species with emission factors >0.01 g kg^{-1} are shown. The order of NMHC species is the same

1012 as Table S1 in which a comprehensive dataset of emission factors measured in this work is

1013 included.

1014

Atmos. Chem. Phys. Discuss., https://doi.org/10.5194/acp-2017-626
Manuscript under review for journal Atmos. Chem. Phys.
Discussion started: 23 August 2017

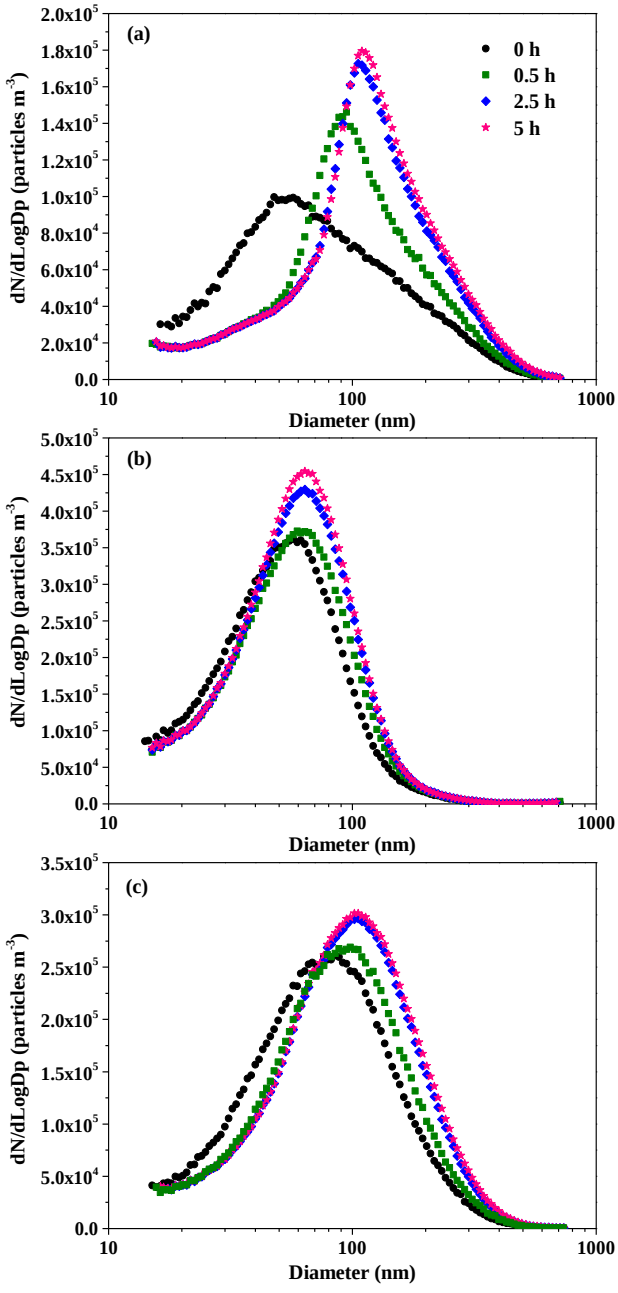

1015

1016 **Figure 3.** Particle size distributions in different burning. (a) Burn 2: rice straw; (b) Burn 3:

1017 corn straw, (c) Burn 5: wheat straw.

Atmos. Chem. Phys. Discuss., https://doi.org/10.5194/acp-2017-626
Manuscript under review for journal Atmos. Chem. Phys.
Discussion started: 23 August 2017

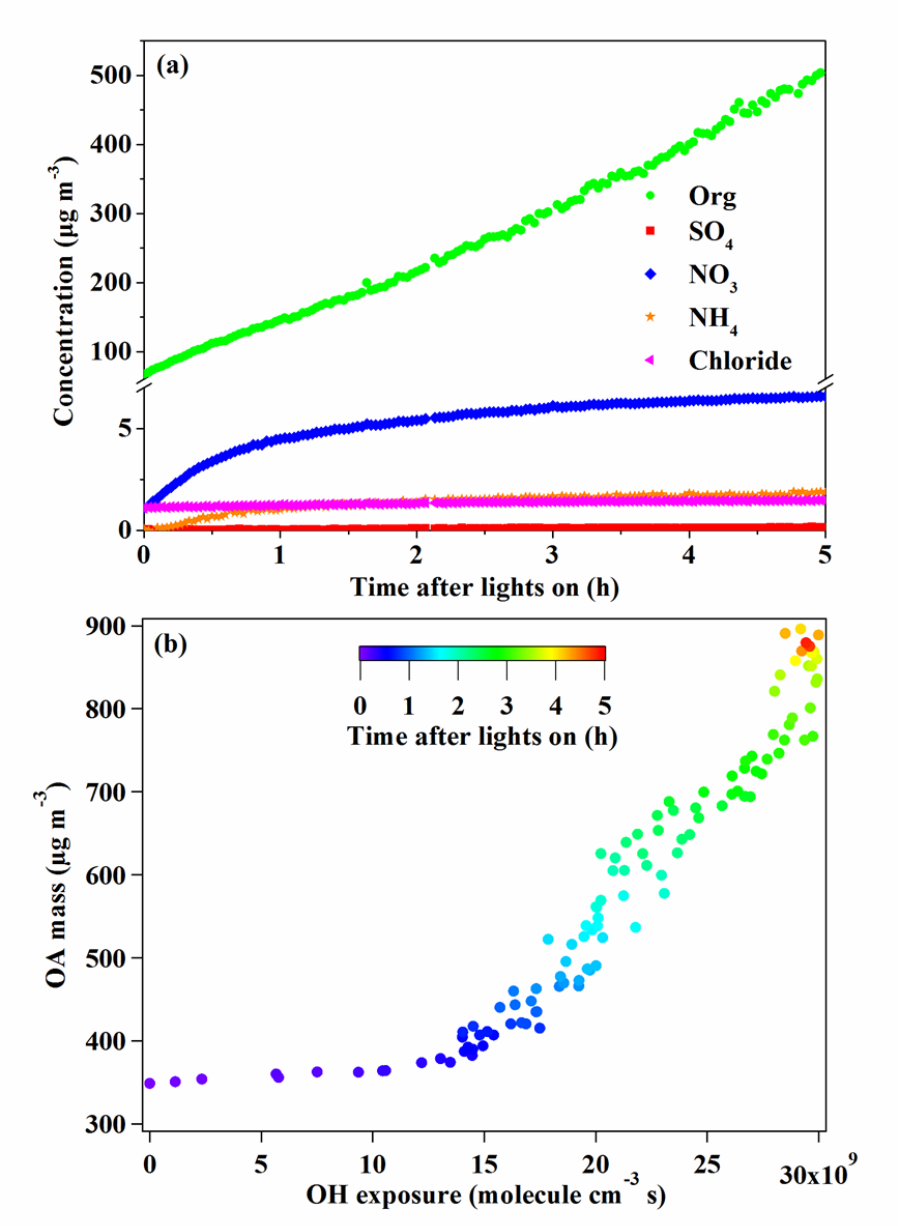

Figure 4. (a) The evolution of particulate matter components (Burn 2). (b) OA mass growth as a function of OH exposure (Burn 5).

Atmos. Chem. Phys. Discuss., https://doi.org/10.5194/acp-2017-626
Manuscript under review for journal Atmos. Chem. Phys.
Discussion started: 23 August 2017

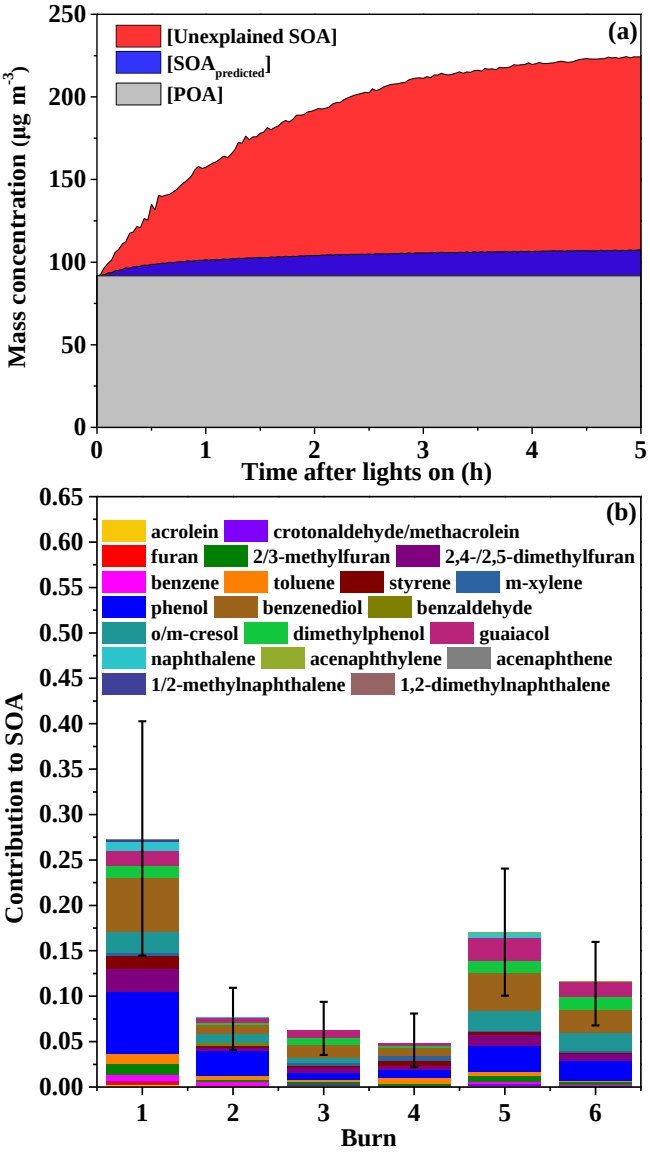

Figure 5. (a) Time series plots of concentrations of POA, secondary organic aerosol that can be explained by the reacted precursors ($SOA_{predicted}$), the difference between the formed SOA and the predicted SOA (Unexplained SOA) in Burn 6. (b) Contribution of 20 NMOGs to the formed SOA at the end of photoreactions. Error bars correspond to the range of contributions when the lowest/highest SOA yields in references were used for all precursors.

Atmos. Chem. Phys. Discuss., https://doi.org/10.5194/acp-2017-626
Manuscript under review for journal Atmos. Chem. Phys.
Discussion started: 23 August 2017

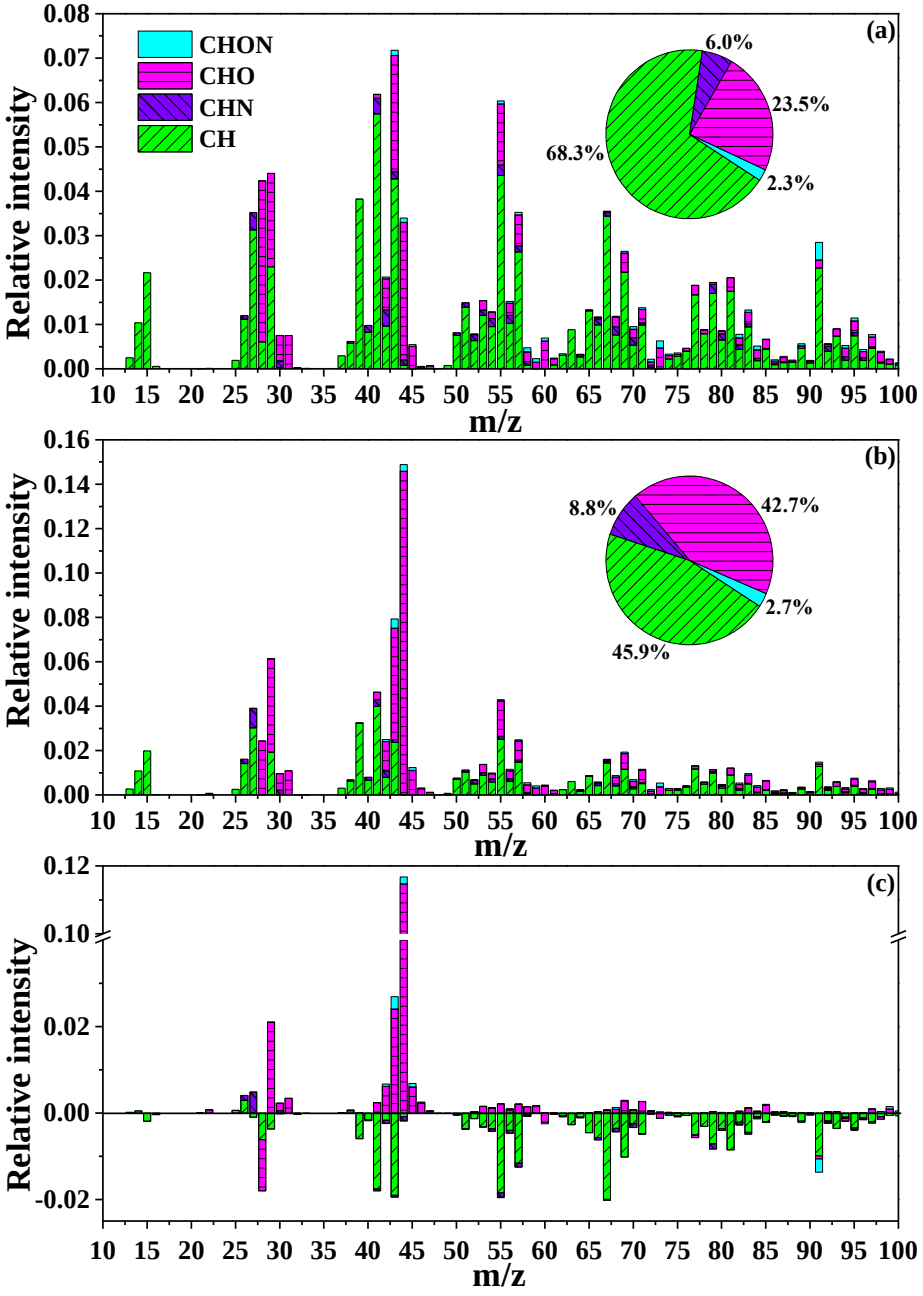

Figure 6. (a) Mass spectrum of POA; (b) mass spectrum of aged OA; (c) Difference in mass spectra between aged OA and POA. The data were all taken from Burn 5.

Atmos. Chem. Phys. Discuss., https://doi.org/10.5194/acp-2017-626
Manuscript under review for journal Atmos. Chem. Phys.
Discussion started: 23 August 2017

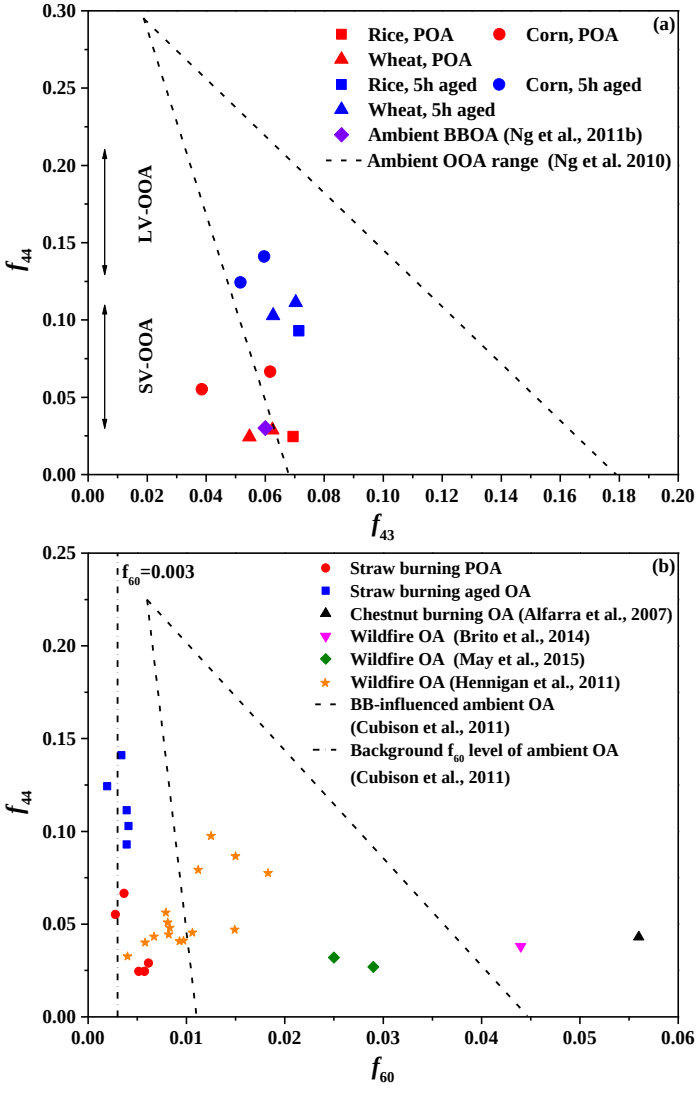

Figure 7. (a) Comparison of f_{44} vs f_{43} determined in our work with those for the ambient BBOA data sets (Ng et al., 2011b) and the ambient OOA range (Ng et al., 2010). The typical f_{44} ranges of ambient SV-OOA and LV-OOA are indicated with the vertical arrows. (b) Comparison of f_{44} vs f_{60} for straw burning OA with those for other types of biomass burning OA (Alfarra et al., 2007; Hennigan et al., 2011; Cubison et al., 2011; Brito et al., 2014; May et al., 2015).

Atmos. Chem. Phys. Discuss., https://doi.org/10.5194/acp-2017-626
Manuscript under review for journal Atmos. Chem. Phys.
Discussion started: 23 August 2017

Atmospheric Chemistry and Physics Discussions

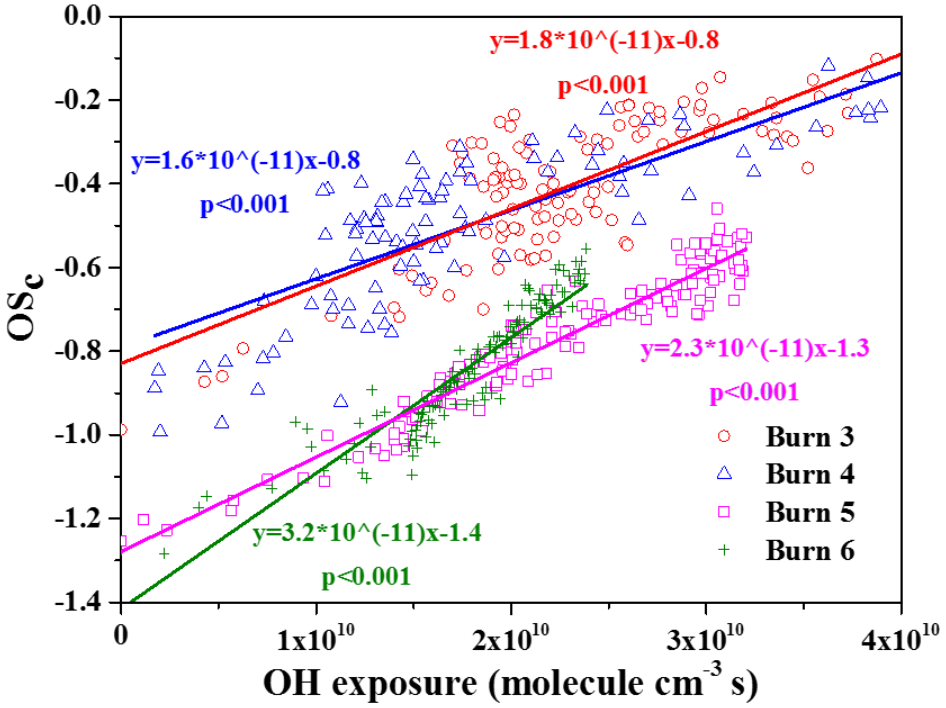

Figure 8. The growth of OA carbon oxidation state with OH exposure for burning corn (Burn 3 and 4) and wheat (Burn 5 and 6) straws. Data for burning rice straws were not included since in Burn 1 AMS was then not run in W-mode.

Atmos. Chem. Phys. Discuss., https://doi.org/10.5194/acp-2017-626
Manuscript under review for journal Atmos. Chem. Phys.
Discussion started: 23 August 2017

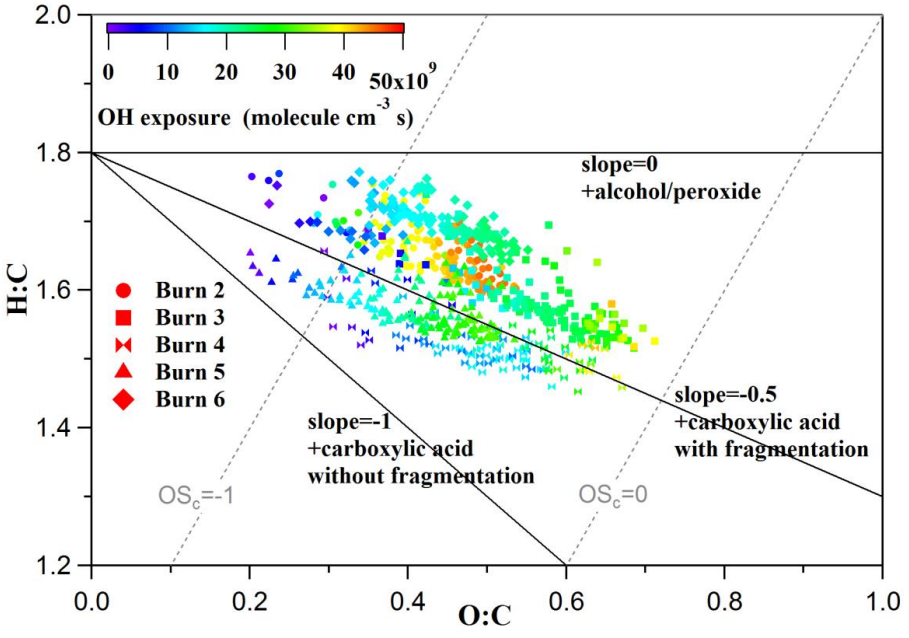

1042

1043 **Figure 9.** Van Krevelen diagram for the OA. Each slope corresponds to the addition of a

1044 specific functional group to an aliphatic carbon.

1045